

X-ray and Laser Spectroscopy on the Oxford EBIT

20 Years of Spectroscopy with the EBIT
Berkeley City Club, 16th November 2006



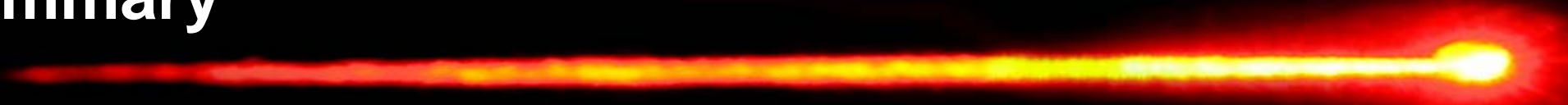




David Crosby

Clarendon Laboratory, University of Oxford

<http://www.physics.ox.ac.uk/ebit>

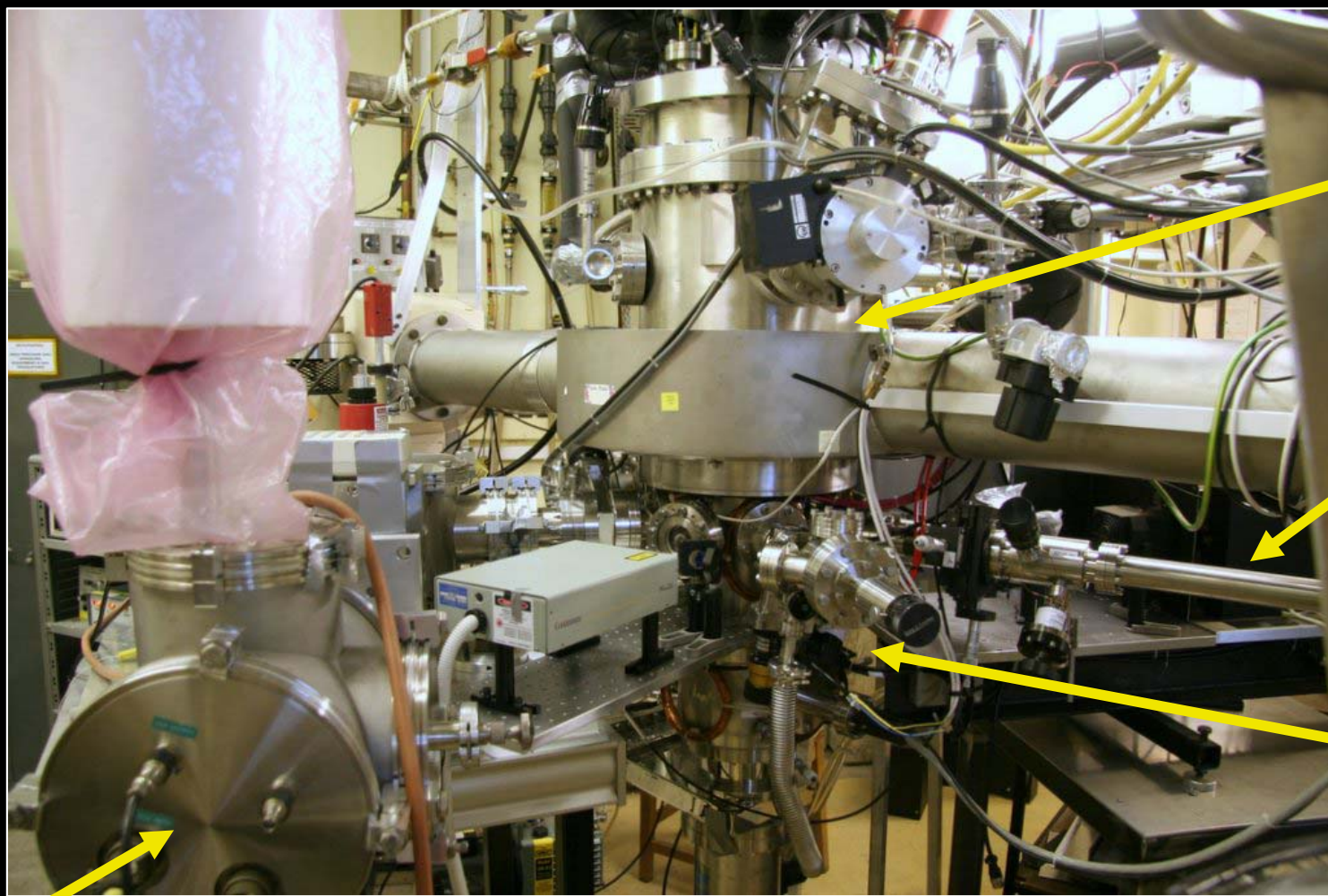


Summary

- 
-  Tests of QED with hydrogen-like ions
 -  Laser spectroscopy of hydrogenlike nitrogen
 -  X-ray spectroscopy of medium Z hydrogenlike ions
 -  Dabbling in EBIT kinetics with a view to the future



The Oxford EBIT



EBIT

Probe

Laser
ablation
atom
source

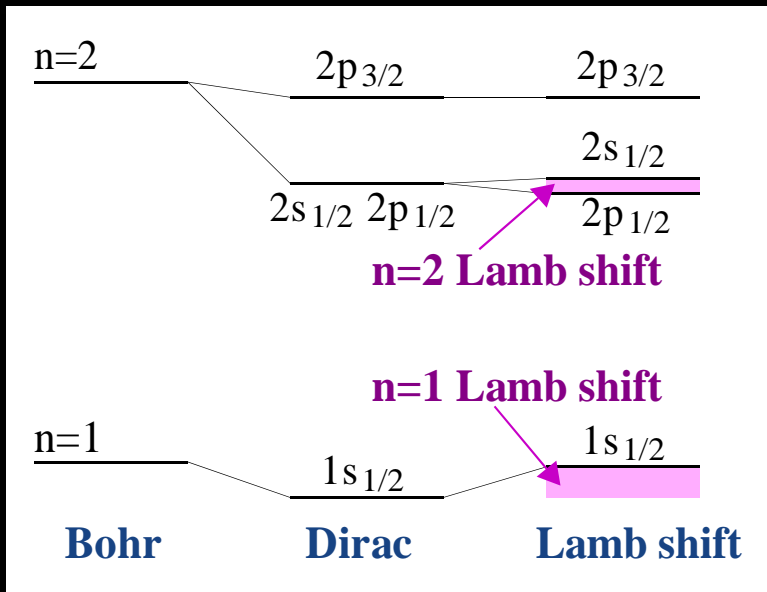
Johann
geometry
X-ray
spectrometer

Carbon dioxide laser

Oxford EBIT Group



Hydrogenic ions & QED



Lamb shift, ΔE

$$\Delta E = \Delta E_{\infty} + \underbrace{\Delta E_{rec} + \Delta E_{RRC}}_{\Delta E_M \text{ [Recoil Corrections]}} + \Delta E_{Nucl}$$

ΔE_{QED} [QED Corrections]

The diagram also shows the contributions to the recoil corrections: Pure Recoil Contribution, Radiative Recoil Contribution, and Influence of the Nuclear Structure.

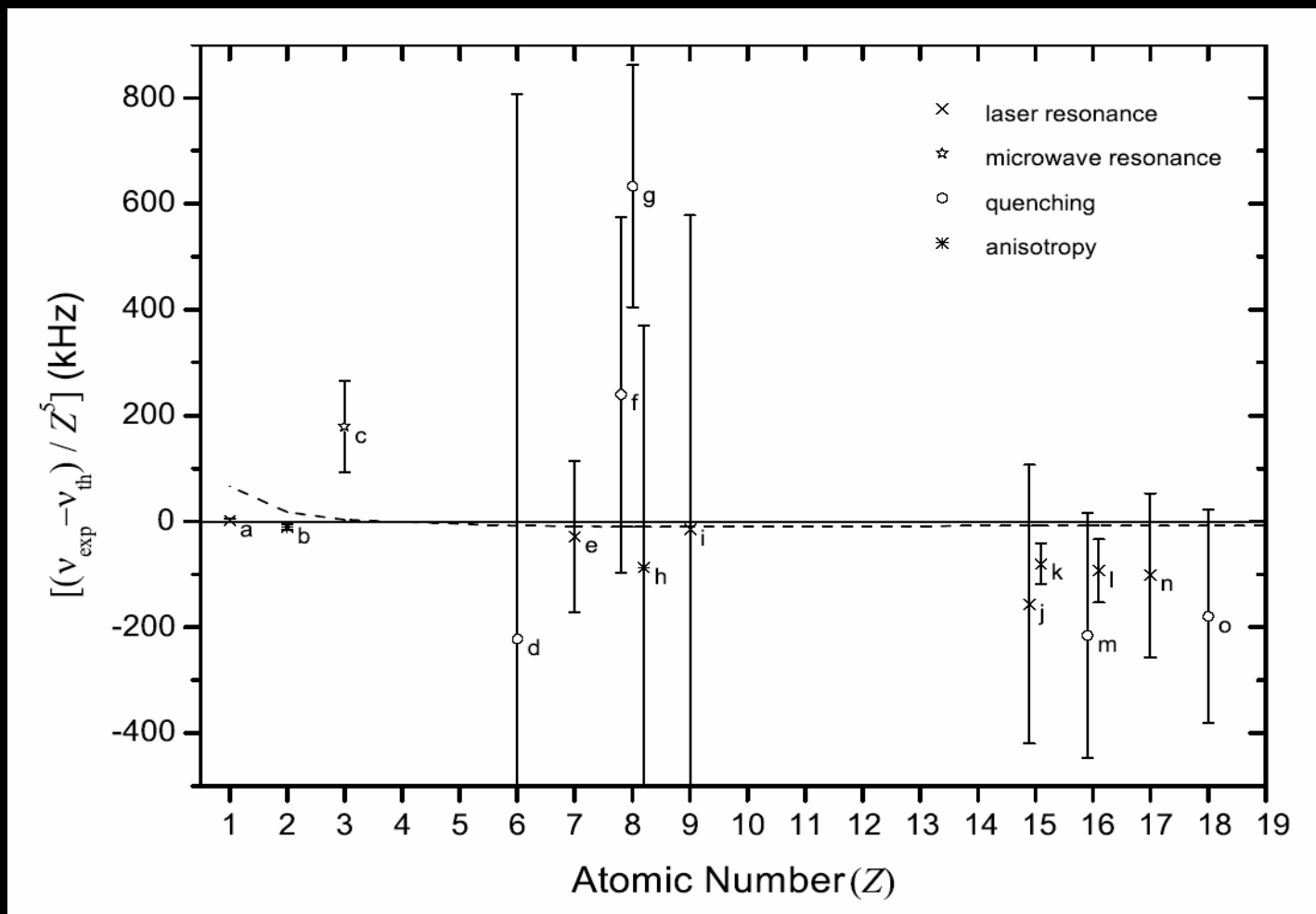
QED contribution found by expansion in $Z\alpha$ (low Z) or numerical calculation (high Z)

$$\Delta E_{\infty} = \frac{\alpha (Z\alpha)^4}{\pi} \left(\frac{m_R}{m} \right) \frac{m}{n^3} \left[\underset{\substack{\uparrow \\ \text{One-loop term}}}{F} + \left(\frac{\alpha}{\pi} \right) \underset{\substack{\uparrow \\ \text{Two-loop term}}}{H} + \left(\frac{\alpha}{\pi} \right)^2 \underset{\substack{\uparrow \\ \text{Three-loop term}}}{K} \right]$$



Experimental target – n=2 Lamb Shift

n=2 Lamb shift measurements

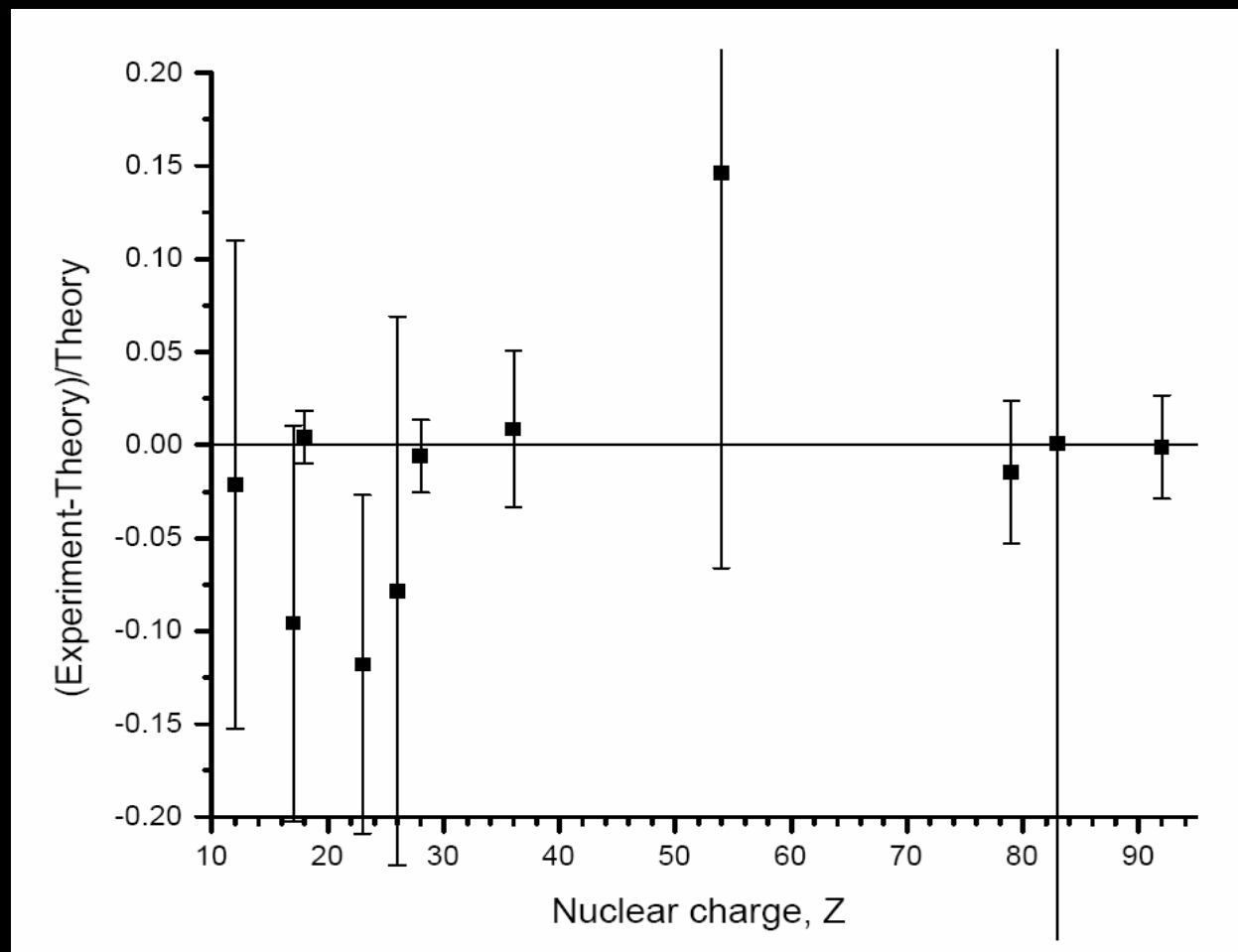


n=2 Lamb shift in N⁶⁺ is 45.41 cm⁻¹, two loop contribution is of order 0.01 cm⁻¹, bulk 2s_{1/2}-2p_{3/2} transition is ~835 cm⁻¹
Target measurement accuracy for transition: <10 ppm,
measurement of Lamb shift to <200 ppm



Experimental target – n=1 Lamb shift

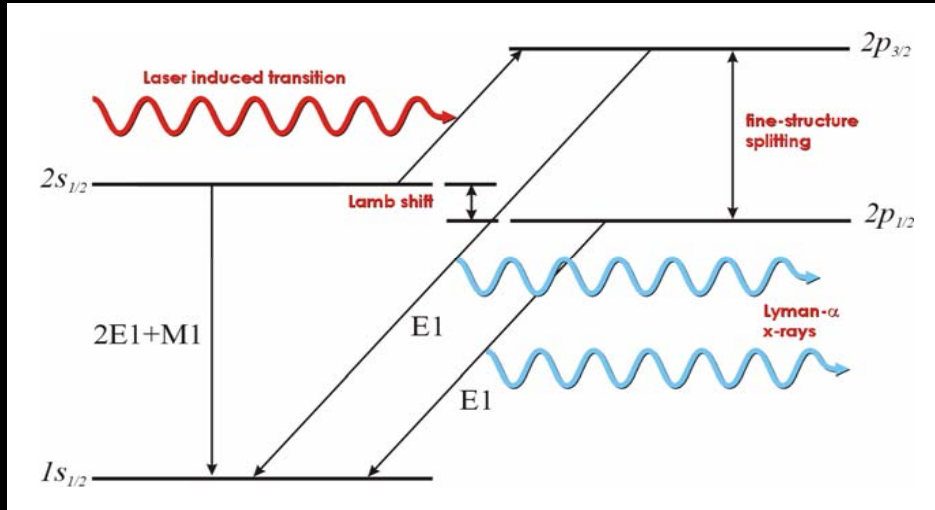
n=1 Lamb shift measurements



$n=1$ Lamb shift in (e.g) Ar^{17+} is 1.141 eV, two loop contribution is of order 0.4 meV, total $1s_{1/2}-2p_{1/2,3/2}$ transitions are at ~ 3320 eV
For two-loop sensitivity measurement target accuracy: <1 ppm

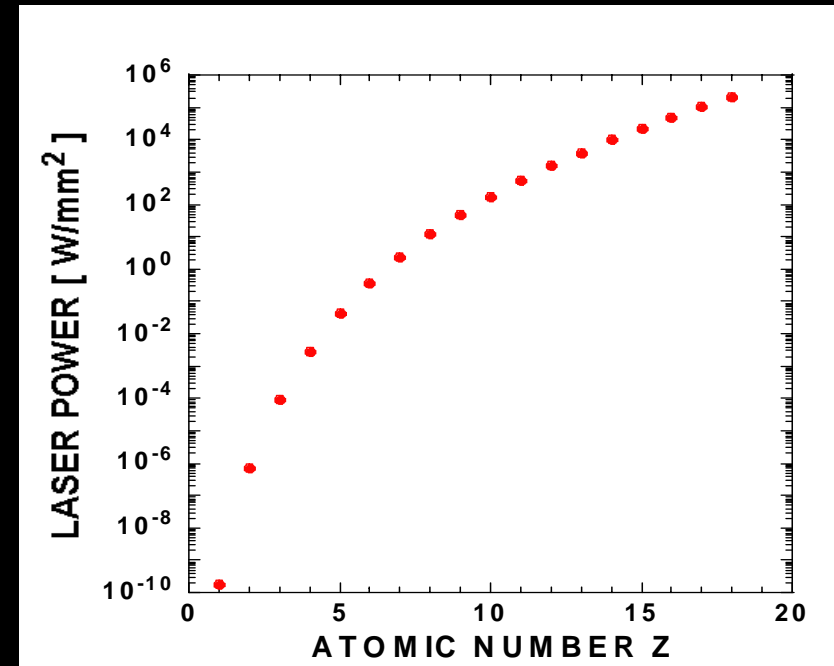


Laser spectroscopy – why Nitrogen?



Laser spectroscopy often dictated by availability of suitable source. With HCl we can use Z to “tune” to suitable sources.

Required laser power to saturate the $2s_{1/2}-2p_{3/2}$ transition as a function of atomic number. Scaling is $\sim Z^{10}$

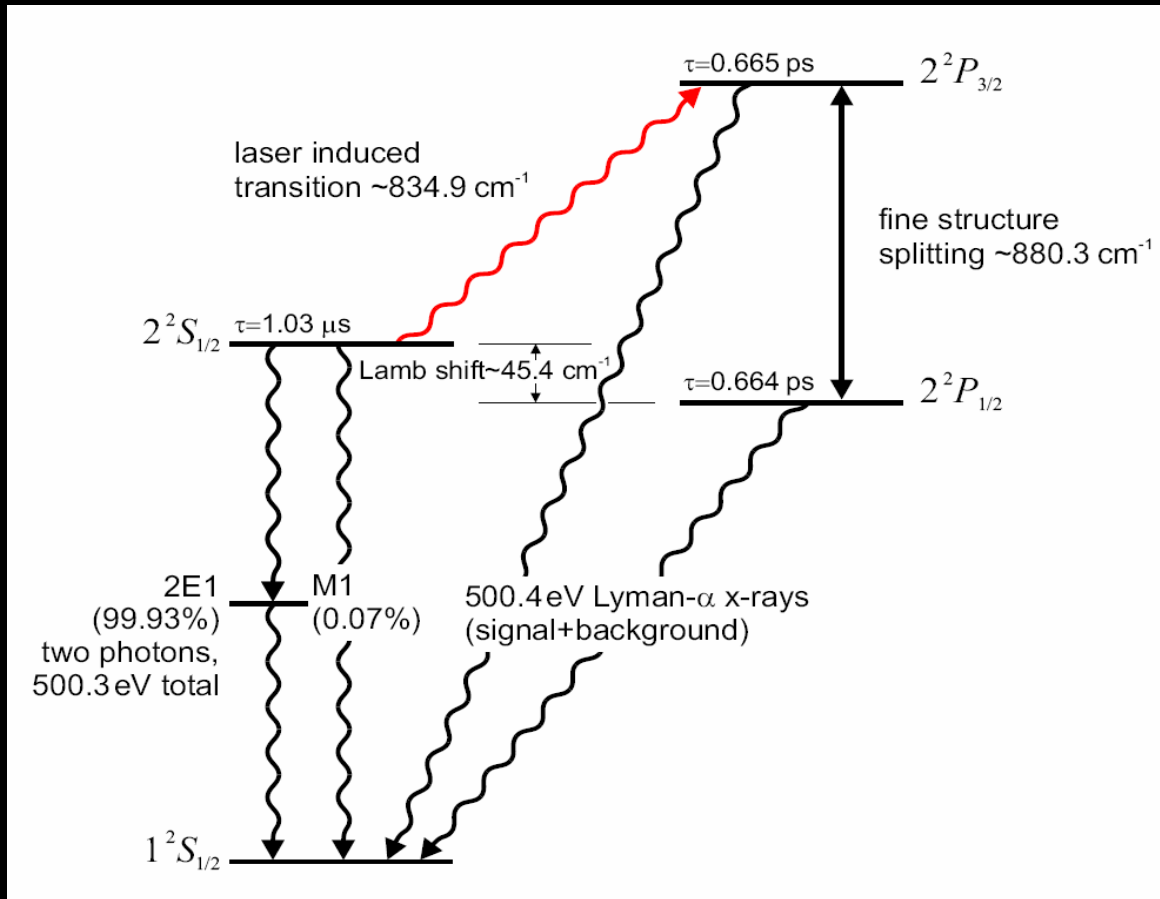


Under saturation conditions, 2.5 W/mm² and 10 kW/mm² are required for N⁶⁺ and Si¹³⁺, respectively.

$2s_{1/2}-2p_{3/2}$ transition in N⁶⁺ happens to overlap the tail of the P-branch of a carbon-14 dioxide laser. The required intensity is easily produced by such a laser.



Laser spectroscopy of N^{6+}



Term diagram for $n=1,2$ levels of N^{6+}

$^{14}\text{C}^{16}\text{O}_2$ laser used to drive transition of electron from $2s_{1/2}$ to $2p_{3/2}$ state.

Electron subsequently decays via E1 emission to ground state. (cf. 2E1 emission from $2s_{1/2}$)

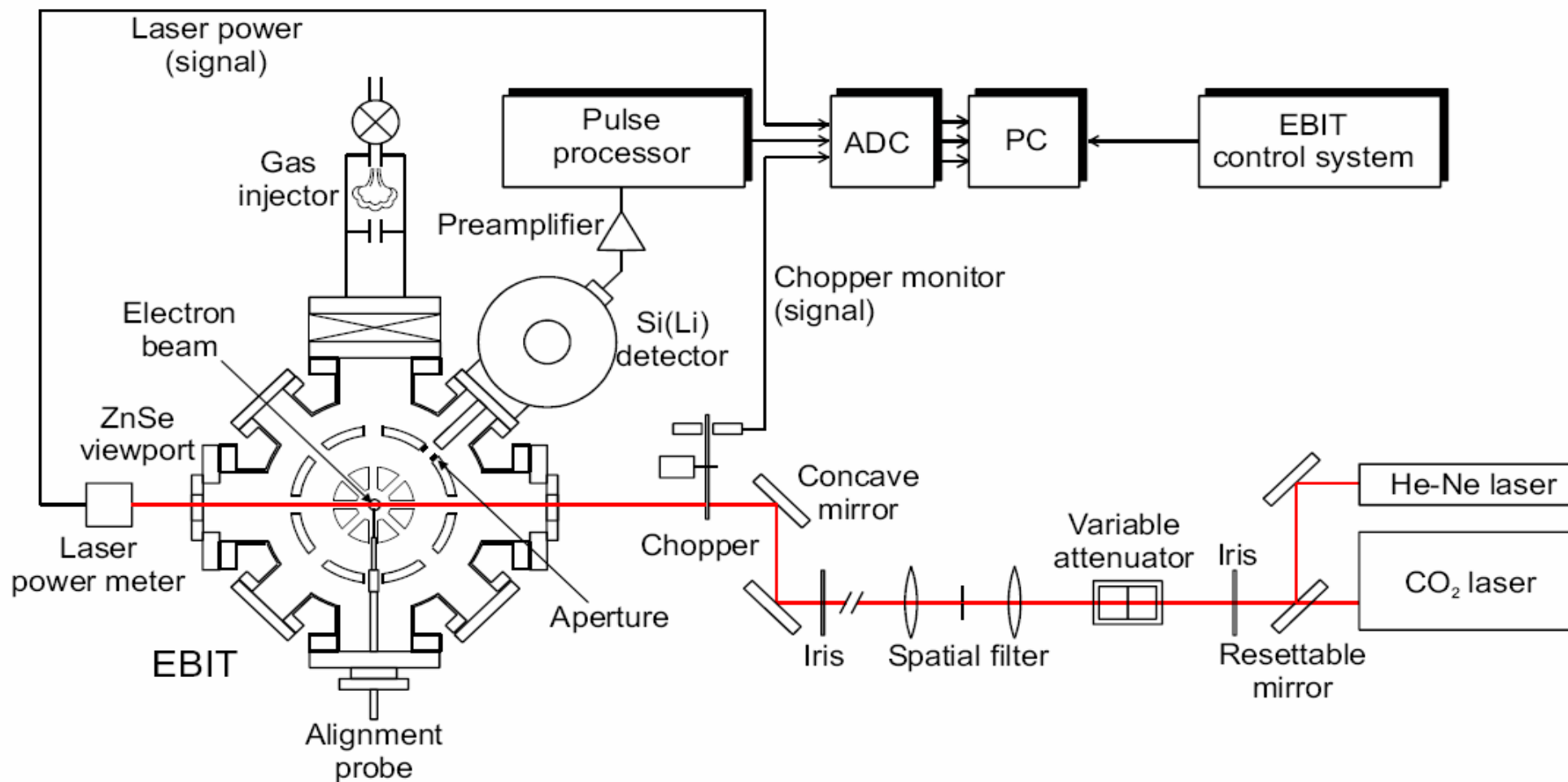
Result is an enhancement in emission of 500 eV photons and a reduction in two photon emission centered at 250 eV.

(measured via energy dispersive spectroscopy using a solid state detector)

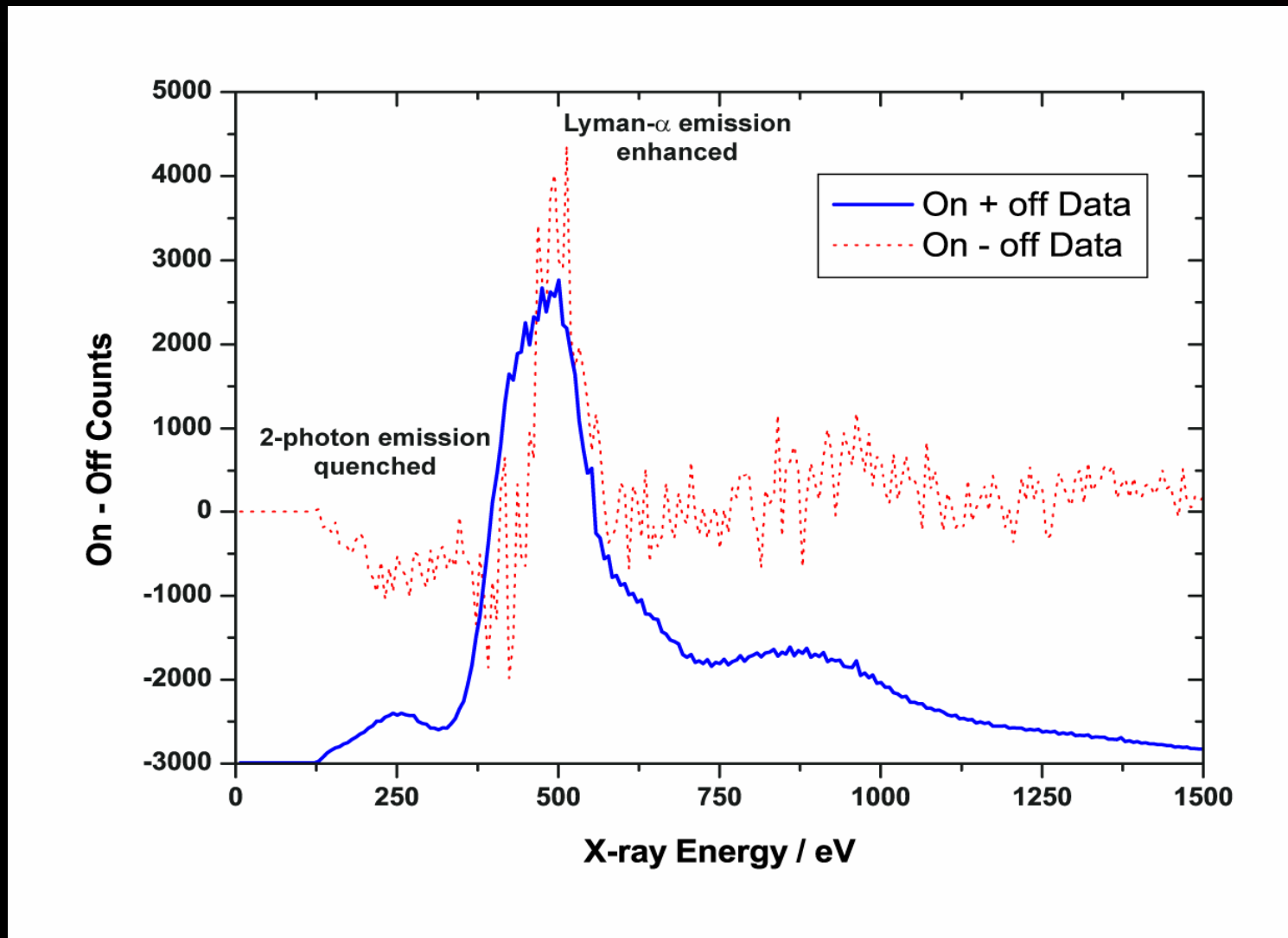
Measure enhancement of x-rays as a function of driving laser wavelength.



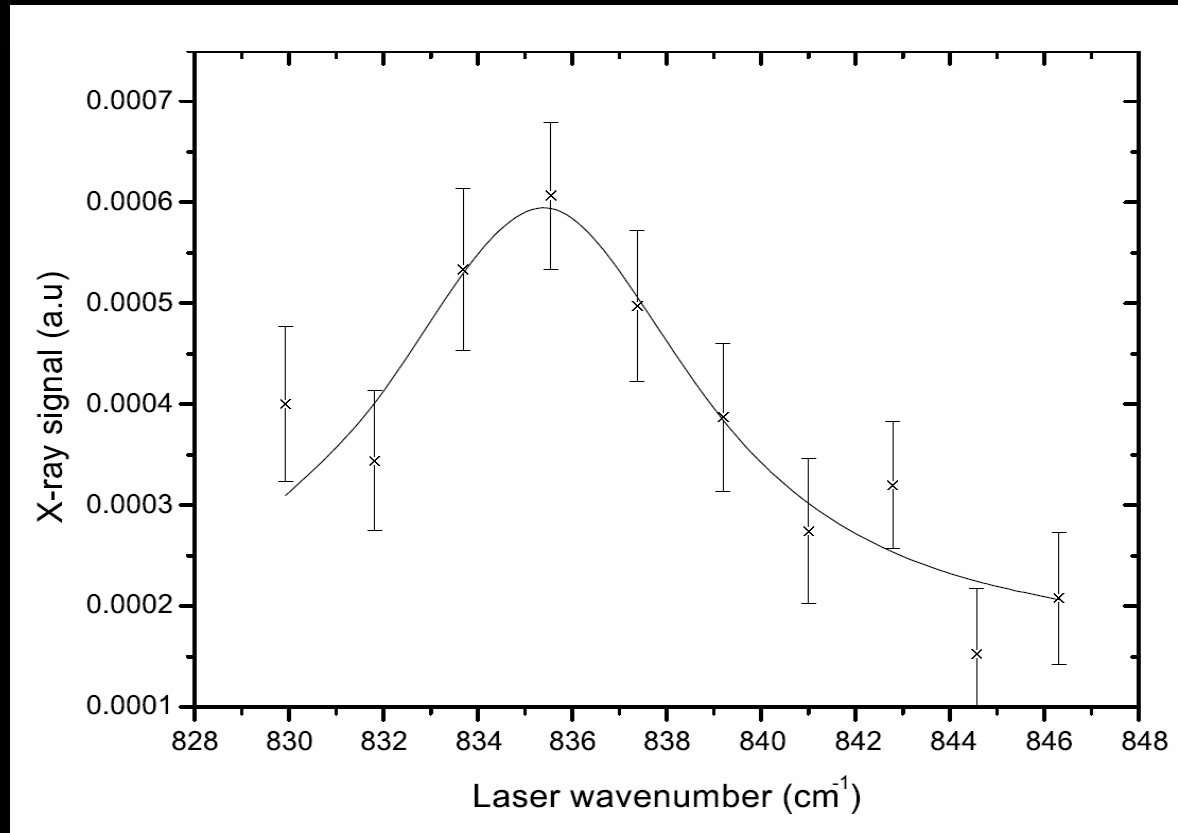
Laser spectroscopy – setup



Laser spectroscopy - results



Laser spectroscopy - results



First successful application of laser spectroscopy to highly charged ions in an electron beam ion trap, result = $835.0 \pm 0.5 \text{ cm}^{-1}$.

Note that the transition is very broad due to lifetime broadening by the short-lived $2p_{3/2}$ state, unlike most spectroscopy measurements on EBIT this dominates over Doppler broadening ($\sim 2\%$).



Laser spectroscopy – developments

Experiment is a factor of 50 short of being “interesting” (0.01 cm^{-1}) and a factor of >100 from being potentially “jolly interesting”

Present limit is experimental statistics – clearly this should be improved:

i) collect more photons:

Improved solid angle and detector efficiency (factor of 50 available)

Measure for longer (perhaps a factor of 10)

ii) improve signal-to-background ratio:

Saturate the transition (build-up cavity)

Exploit motion of the ions through the interaction region

Switch the beam on and off rapidly
(remove large background emission from directly excited $2p_{3/2}$)





Laser spectroscopy – developments II




An “interesting measurement” requires determining centroid to approximately $1/1000$ of linewidth.

There exists considerable potential for systematic errors.

 Laser beam power measurement – with precise bolometers relative precision of $<0.1\%$ possible.

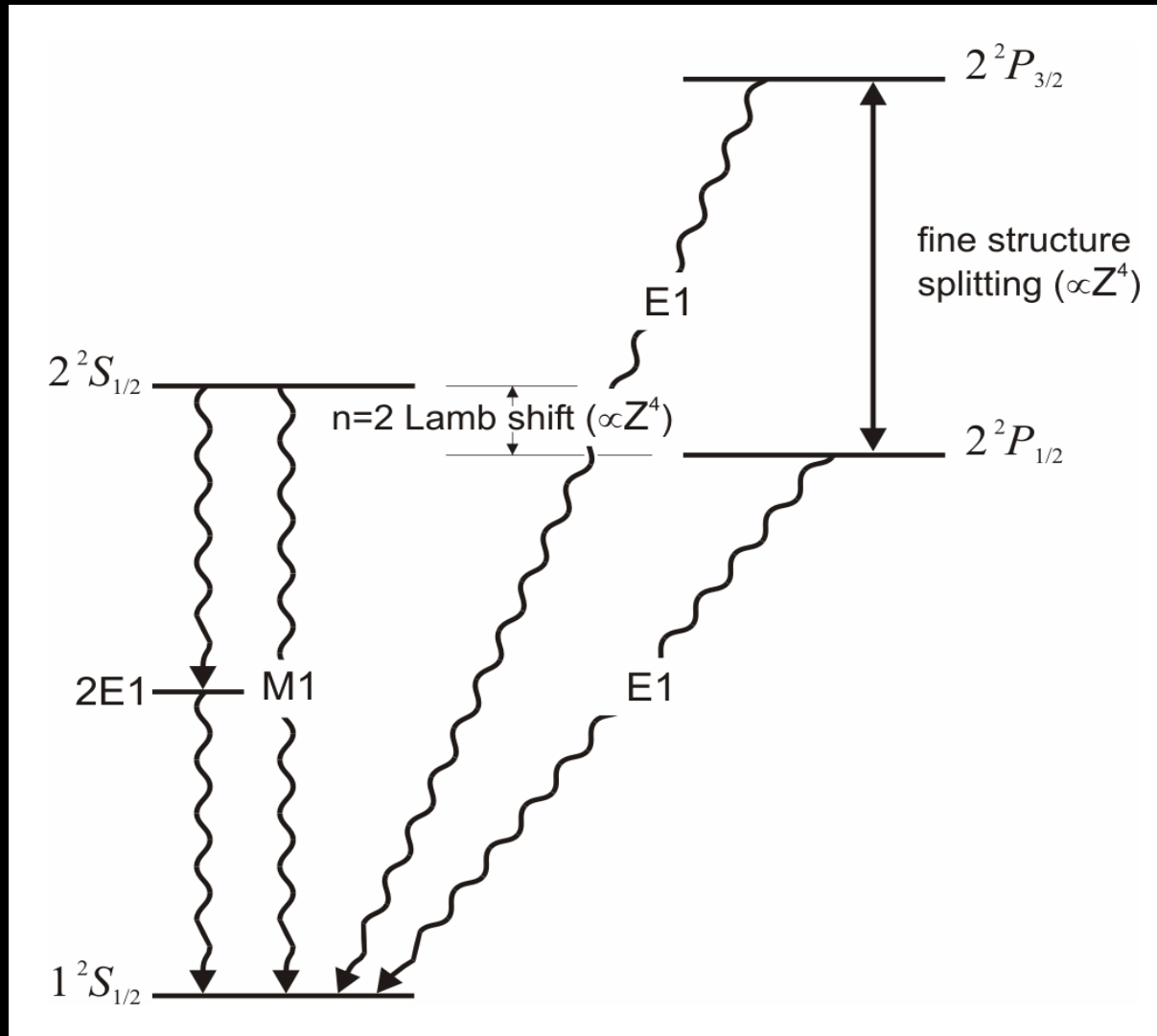
 Laser profile at ion interaction region must also be characterized with similar precision.

 Variations in trap conditions – use total spectrum and imaging as online diagnostic. Ideally use higher a higher resolution detector (Fano limit for silicon should allow factor of ~ 2.5 improvement)

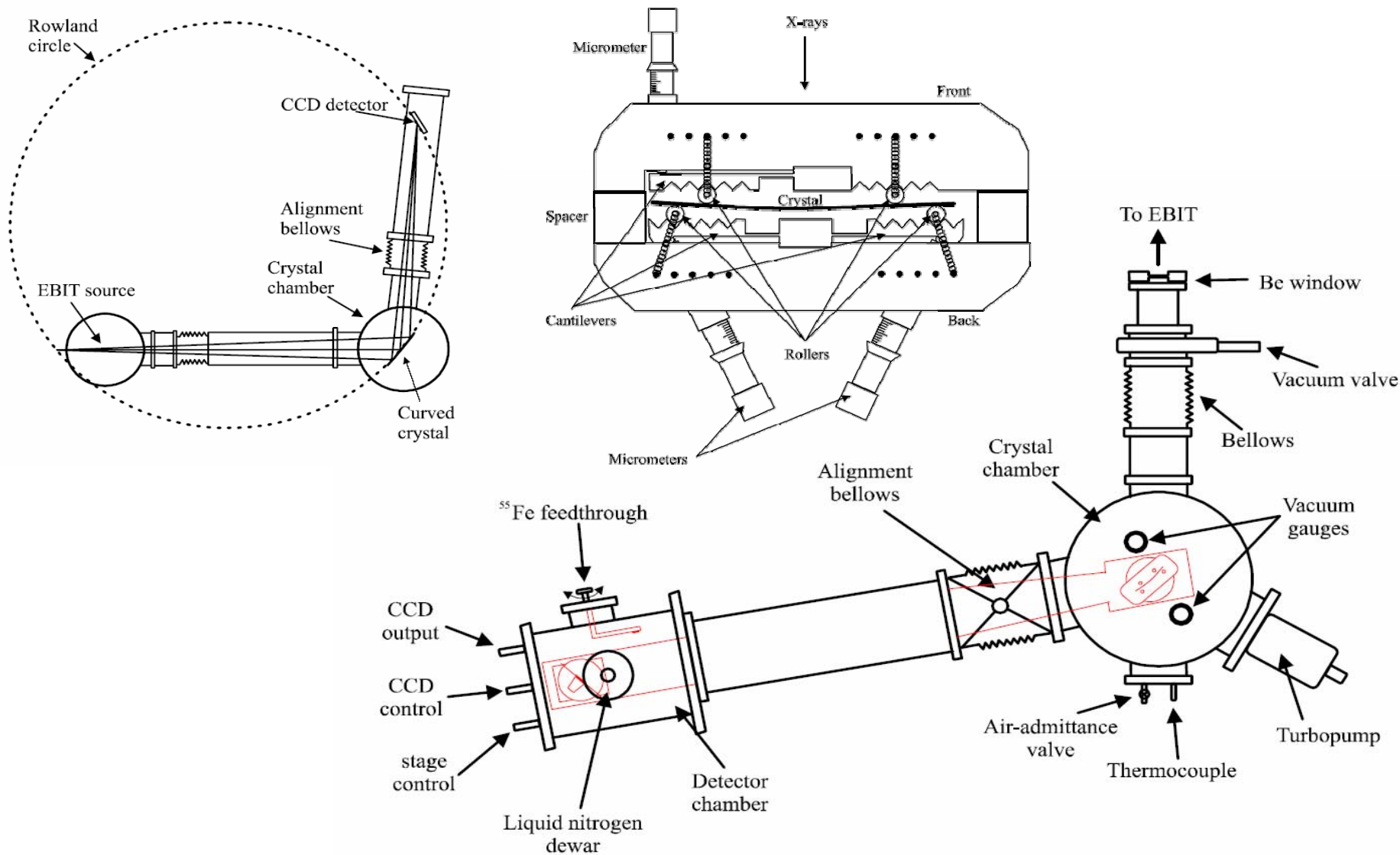


n=1 Lamb shift by emission spectroscopy

Systems of intermediate Z ($\sim 18-36$) represent an interesting region between the regimes of QED calculation by $Z\alpha$ -expansion (low- Z) and numerical calculation (high- Z)



Oxford Johann geometry X-ray spectrometer



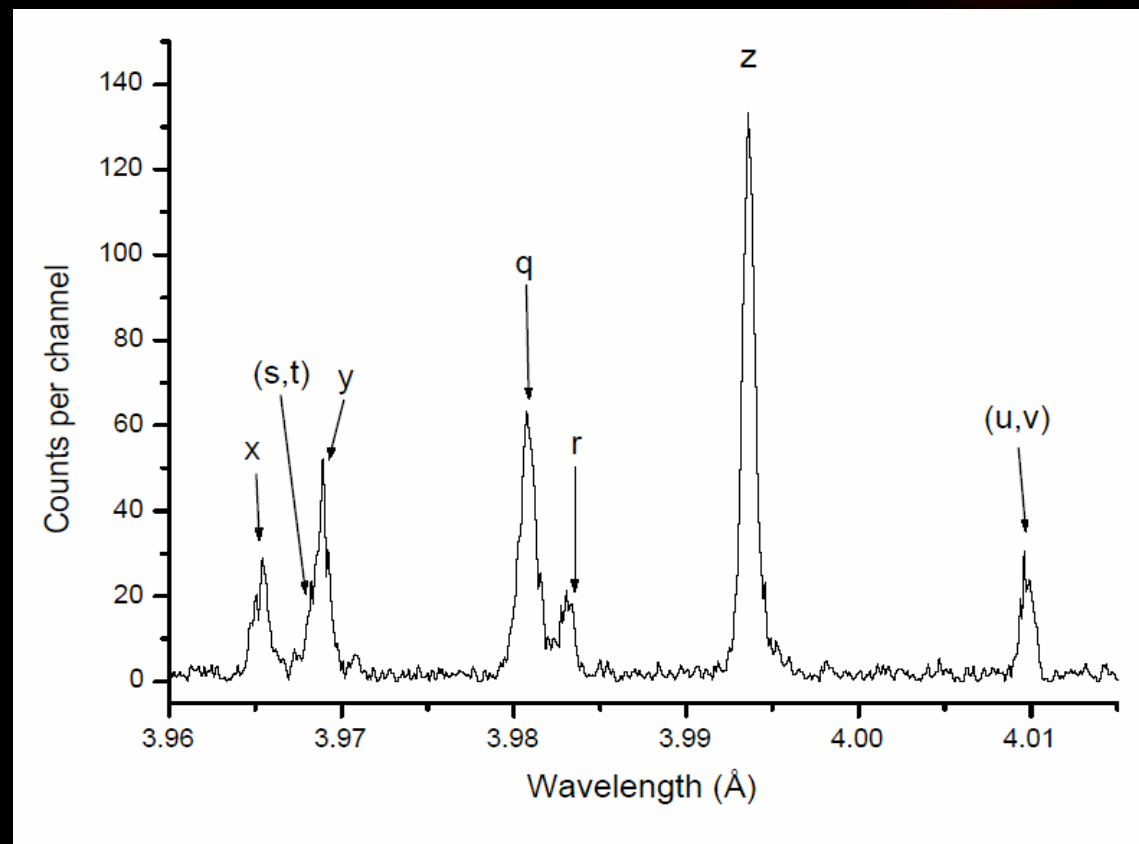
Oxford Johann geometry X-ray spectrometer

Superior resolution and photon collection efficiency

EBIT source must be located sufficiently far inside Rowland circle to provide necessary bandwidth

Absolutely calibrated measurements using crystal lattice spacing not practicable at highest precision due to effects of crystal curvature

Instead calibration requires some secondary wavelength standard – difficult at x-ray wavelengths

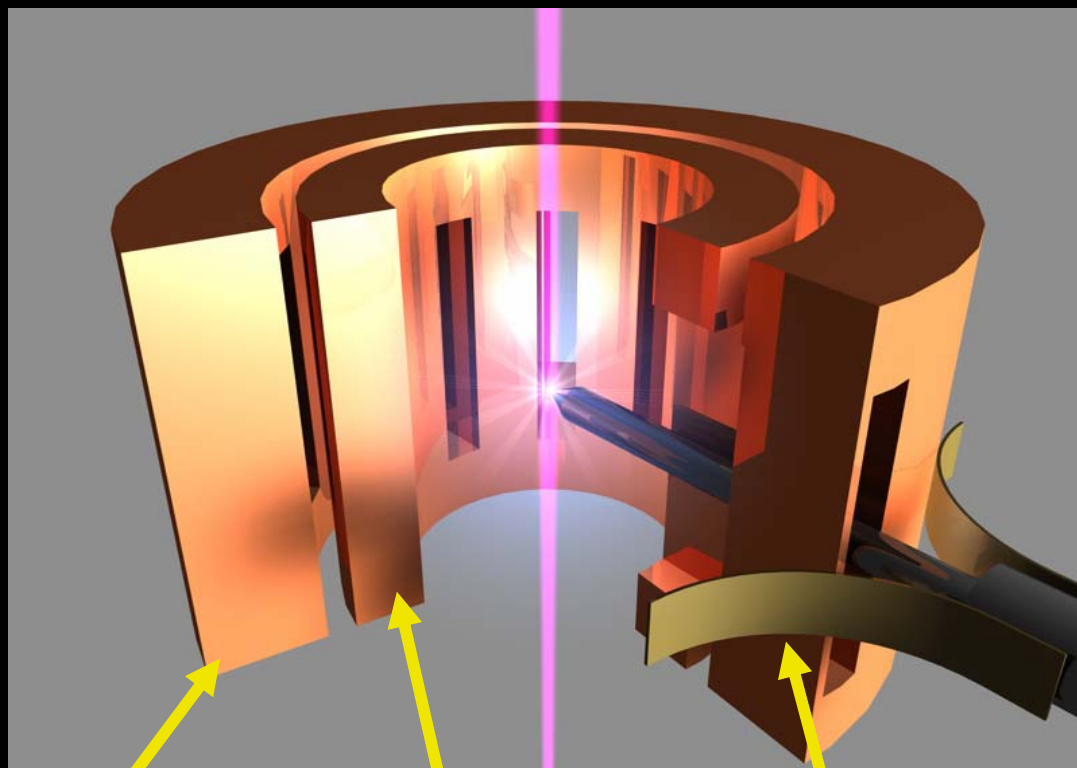


Direct excitation of Ar^{16+} and inner shell excitation of Ar^{15+} , beam energy of 4.1 keV, current of 50 mA. (integration time 160 minutes)



In-situ x-ray calibration

Use wire probe inserted into the electron beam as a source of characteristic $K\alpha$ x-rays

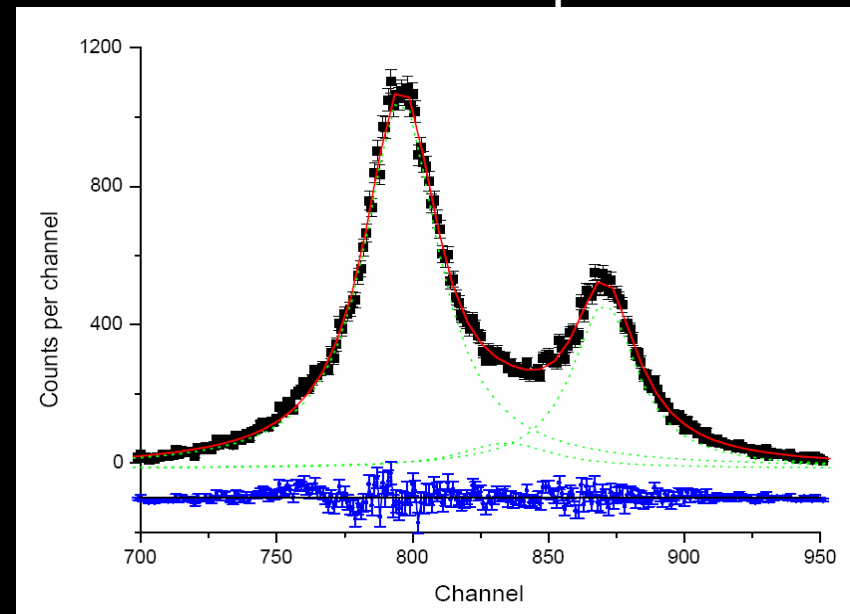


Shield

Drift tube

Electrical and thermal
connection to shield

Vanadium $K\alpha$ calibration spectrum



Other Approaches – Use $2d \sin \theta = n \lambda$:

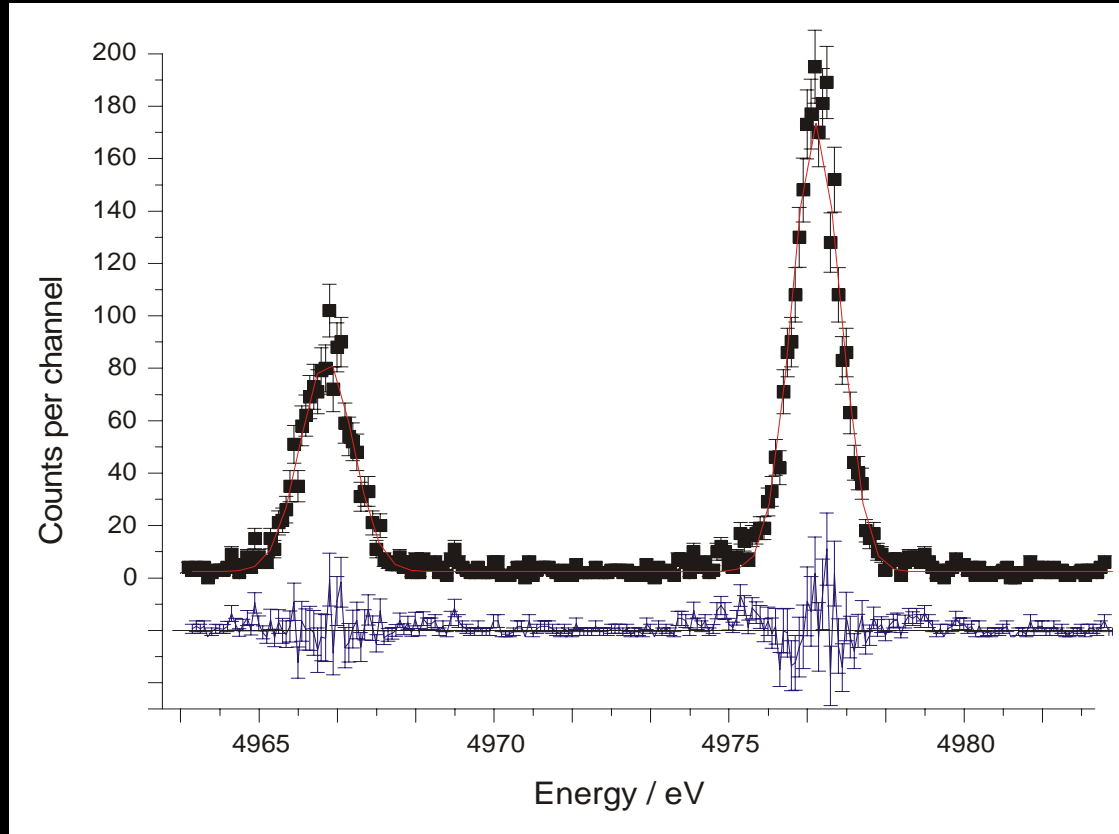
Hölzer *et al.*, Phys. Rev. A, 57, 945 (LLNL, monolithic crystal)

Braun *et al.*, Rev. Sci. Instrum., 76, 073105 (Heidelberg, two crystal comparison)



X-ray spectroscopy – Ti²¹⁺

Hydrogenlike Titanium $1s_{1/2}$ - $2p_{1/2,3/2}$ spectrum



Statistical quality of data sufficient to justify measurement accuracy at the parts-per-million (ppm) level.

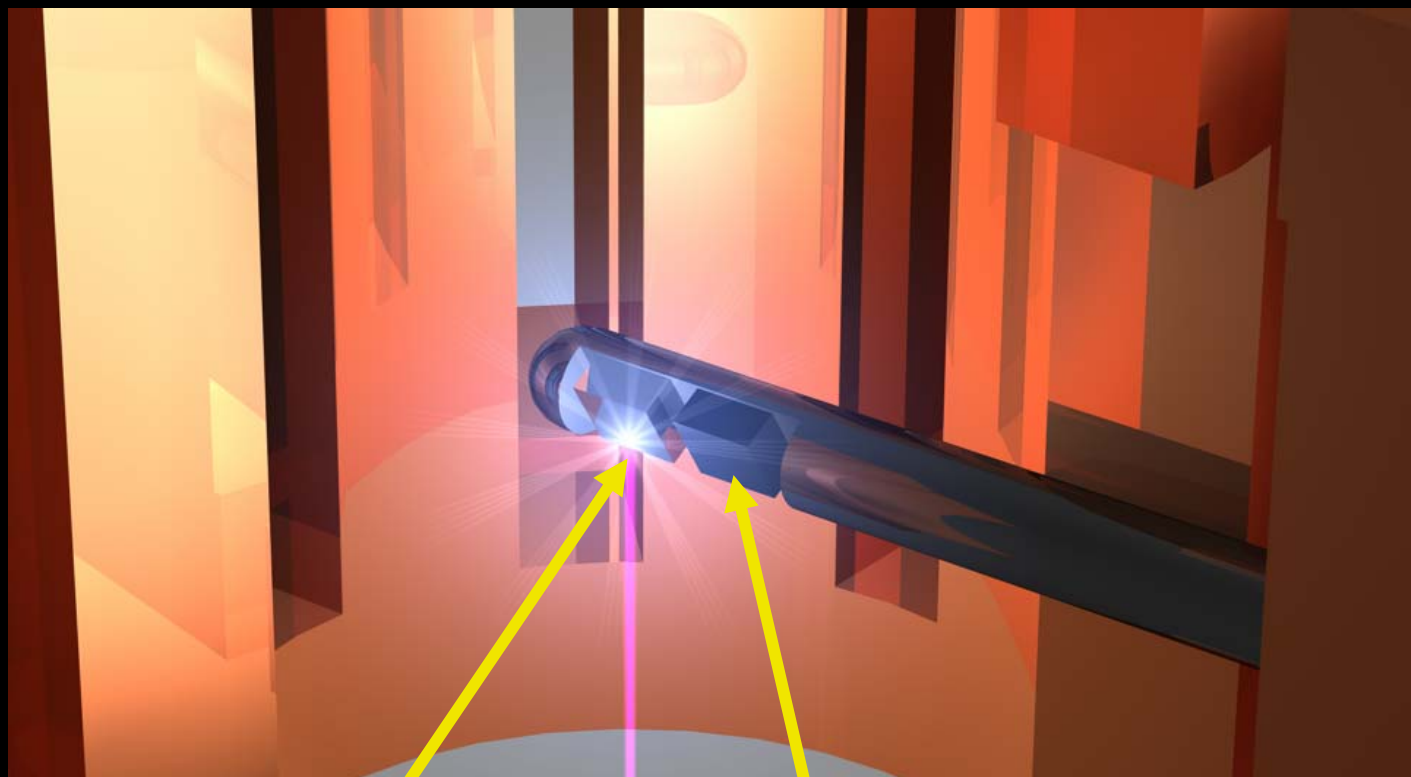
However, overall measurement is only precise to ~20 ppm primarily due to calibration uncertainties.



Improved x-ray calibration



Holzer *et al.*, Phys. Rev. A, 56, 4554 shows that <1 ppm calibration reference is possible, in principle.



Element 1

Element 2

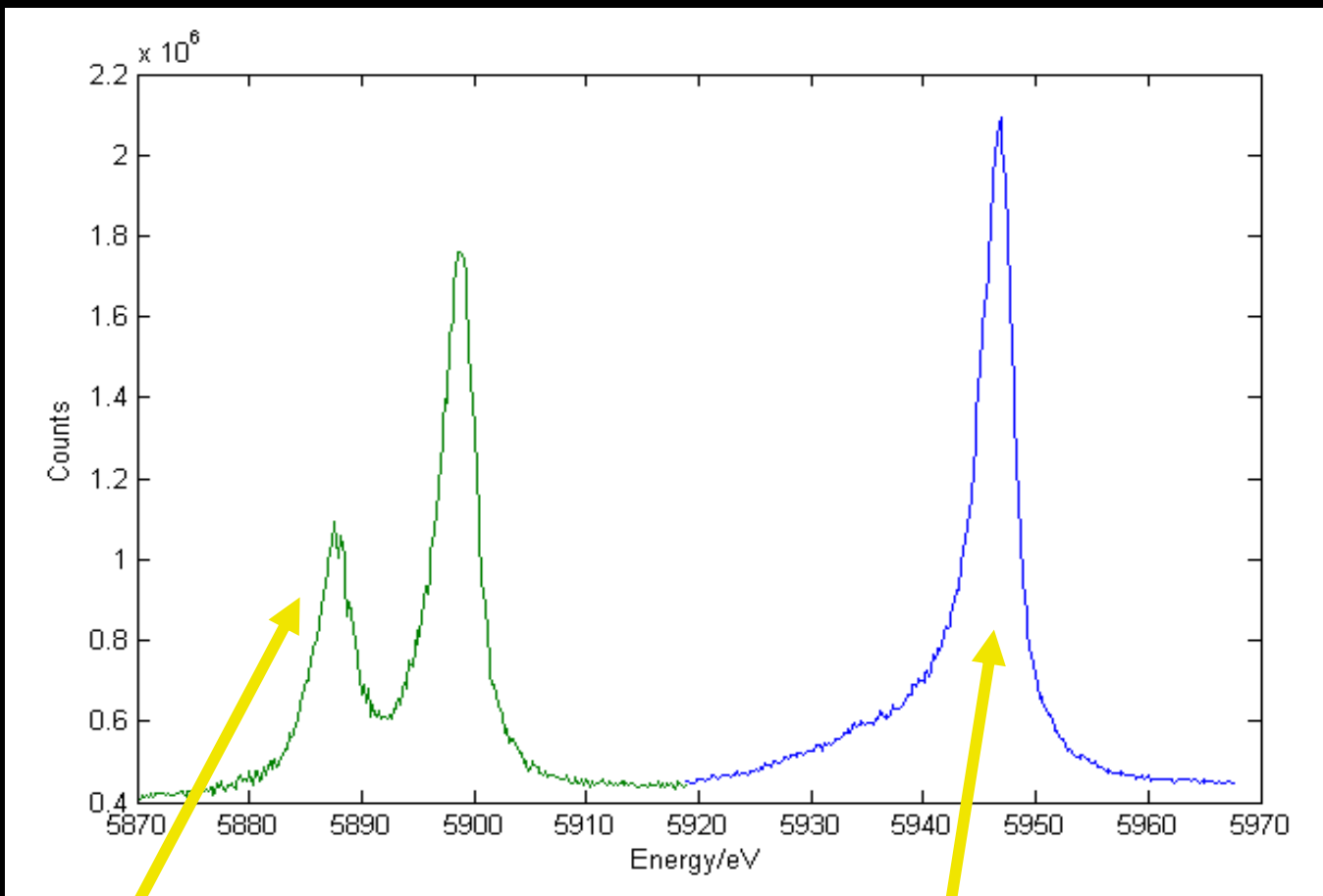
Use probe with planar targets of two different elements - use $K\alpha$ x-rays from element of Z and $K\beta$ x-rays from element of $Z-1$.

This provides more calibration lines, spans the measurement of interest, and controls the x-ray production geometry.



Improved x-ray calibration

Holzer *et al.*, Phys. Rev. A, 56, 4554 shows that <1 ppm calibration reference is possible, in principle.



Element 1,
Manganese $K\alpha_{1,2}$

Element 2,
Chromium $K\beta$



Improved x-ray calibration

Holzer *et al.*, Phys. Rev. A, 56, 4554 shows that <1 ppm calibration reference is possible, in principle. Broad, blended, asymmetric spectral profiles – rather than line centroid from curve fits must use curve peaks

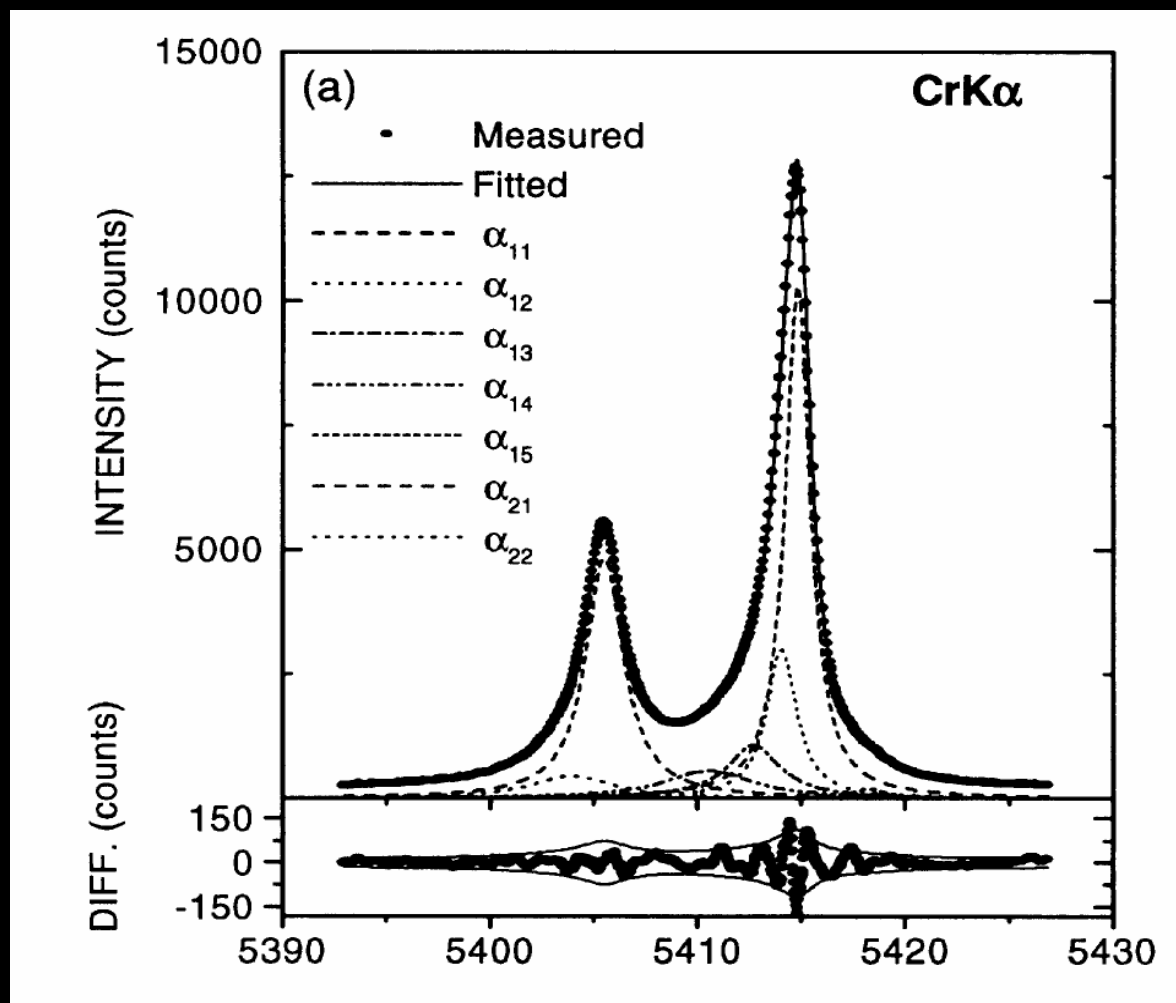
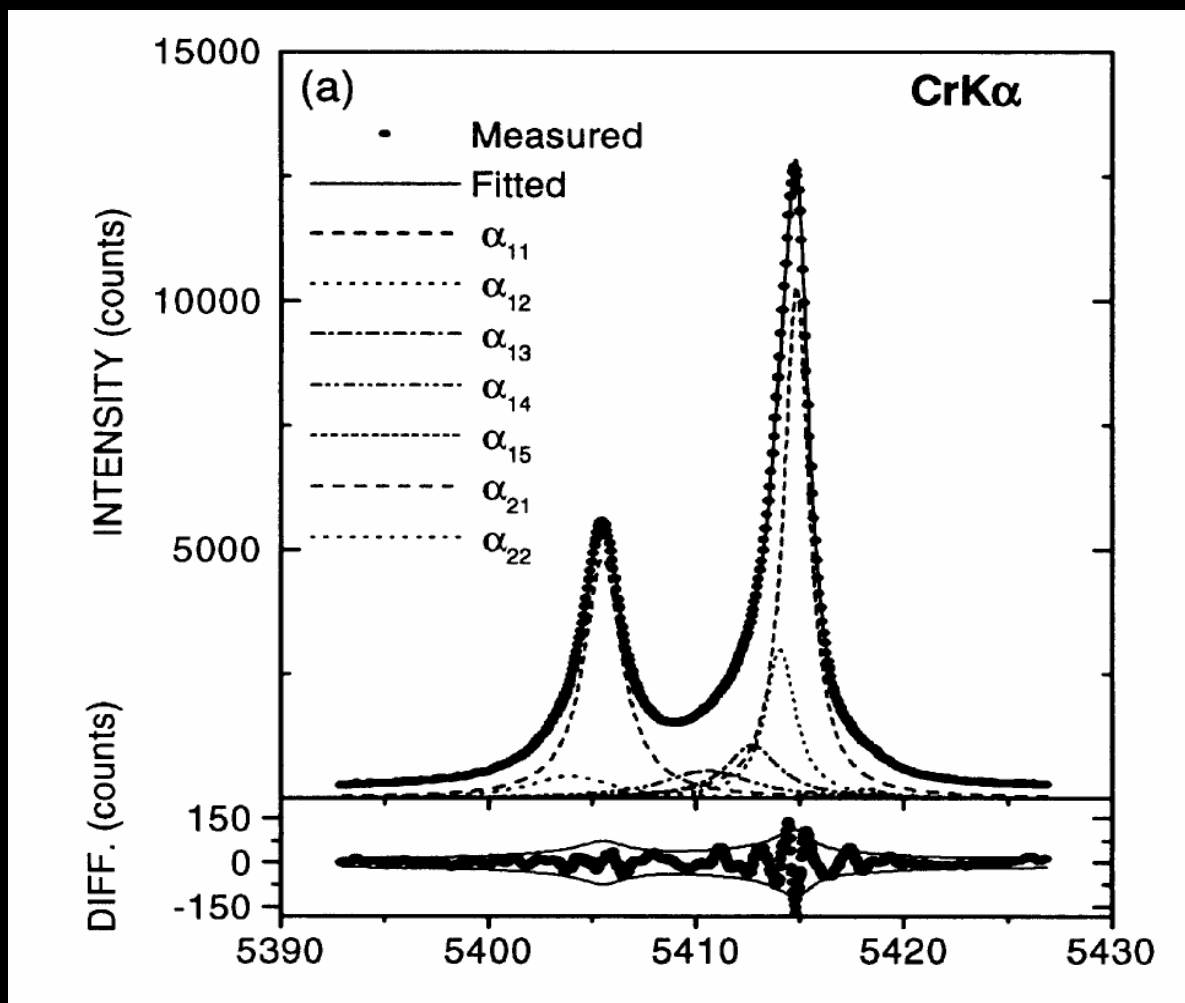


figure from Holzer *et al.*, Phys. Rev. A, 56, 4554



Improved x-ray calibration – issues

Holzer *et al.*, Phys. Rev. A, 56, 4554 shows that <1 ppm calibration reference is possible, in principle. Broad, blended, asymmetric spectral profiles – rather than line centroid from curve fits must use curve peaks



Systematic Effects include:

Difference in illumination geometry (line source for ions, point source for calibration source)

Chemical shifts in source


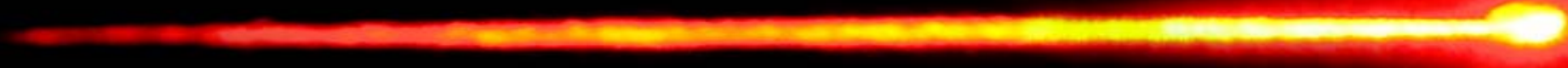
Uncertainties in the shape of the curved crystal

Differences in polarization – can cause shifts due to differences in rocking curves

Convolution shifts



Improved x-ray calibration – issues



Broad, blended, asymmetric spectral profiles – rather than line centroid from curve fits must use curve peaks

Systematic Errors include:

Simulated by raytracing - negligible



Difference in illumination geometry (line source for ions, point source for calibration source)

Being evaluated



Chemical shifts in source, self absorption in source

Crystal surface optically profiled.
Crystal reflections – preliminary observations show that our dispersion function is smooth and accurately approximated



Uncertainties in the shape of the curved crystal

Even pathological differences in polarized output leads to shifts at ~1 ppm level



Differences in polarization – can cause shifts due to differences in rocking curve profiles for σ and π polarization



Improved x-ray calibration – convolution shifts

Convolution shifts – the asymmetric nature of the K x-ray spectrum means that instrumental broadening also leads to a shift of the *peak* position.

See Chantler *et al.*, Phys. Rev. A, 73,012508

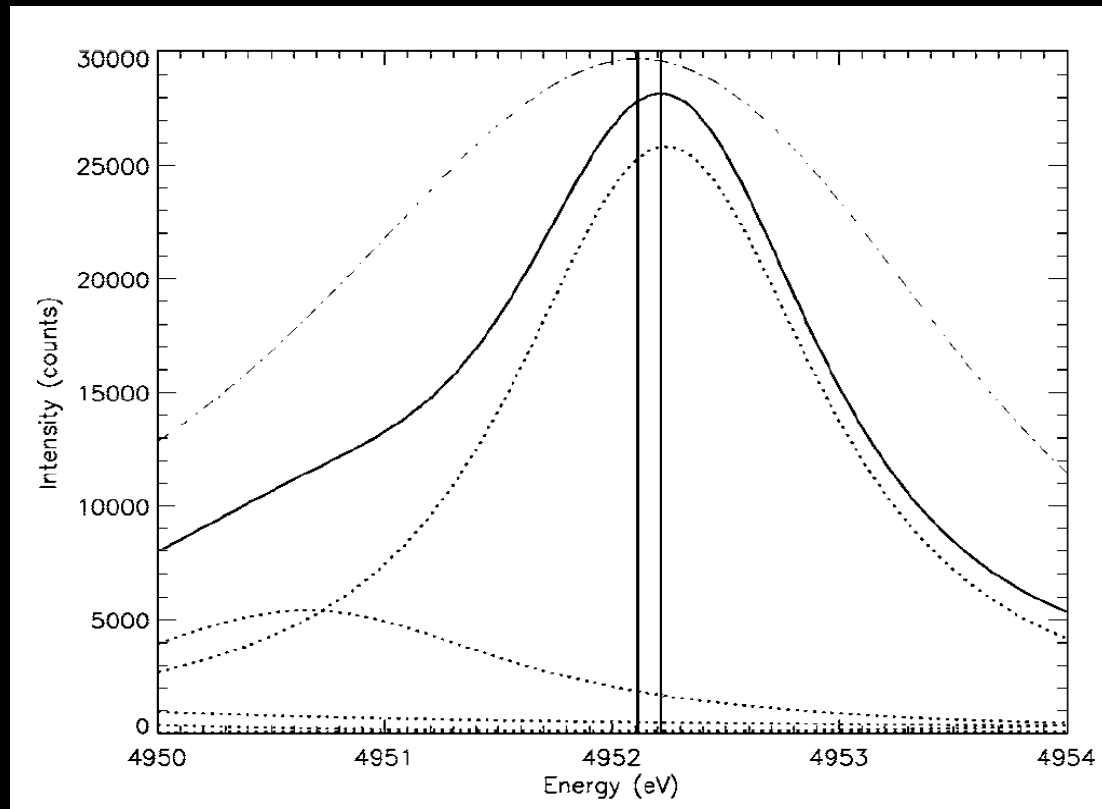
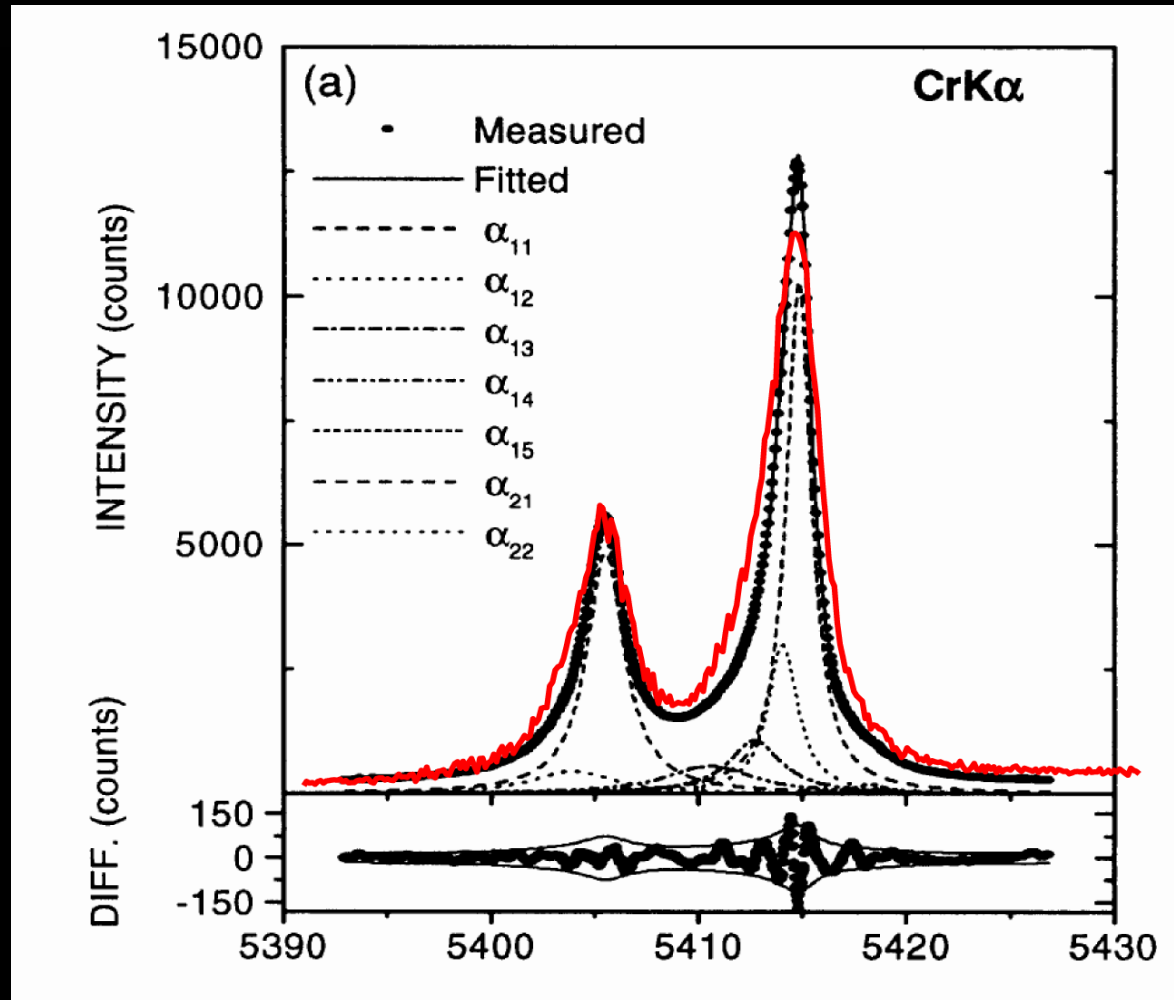


figure from Chantler *et al.*, Phys. Rev. A, 73,012508



Improved x-ray calibration – convolution shifts

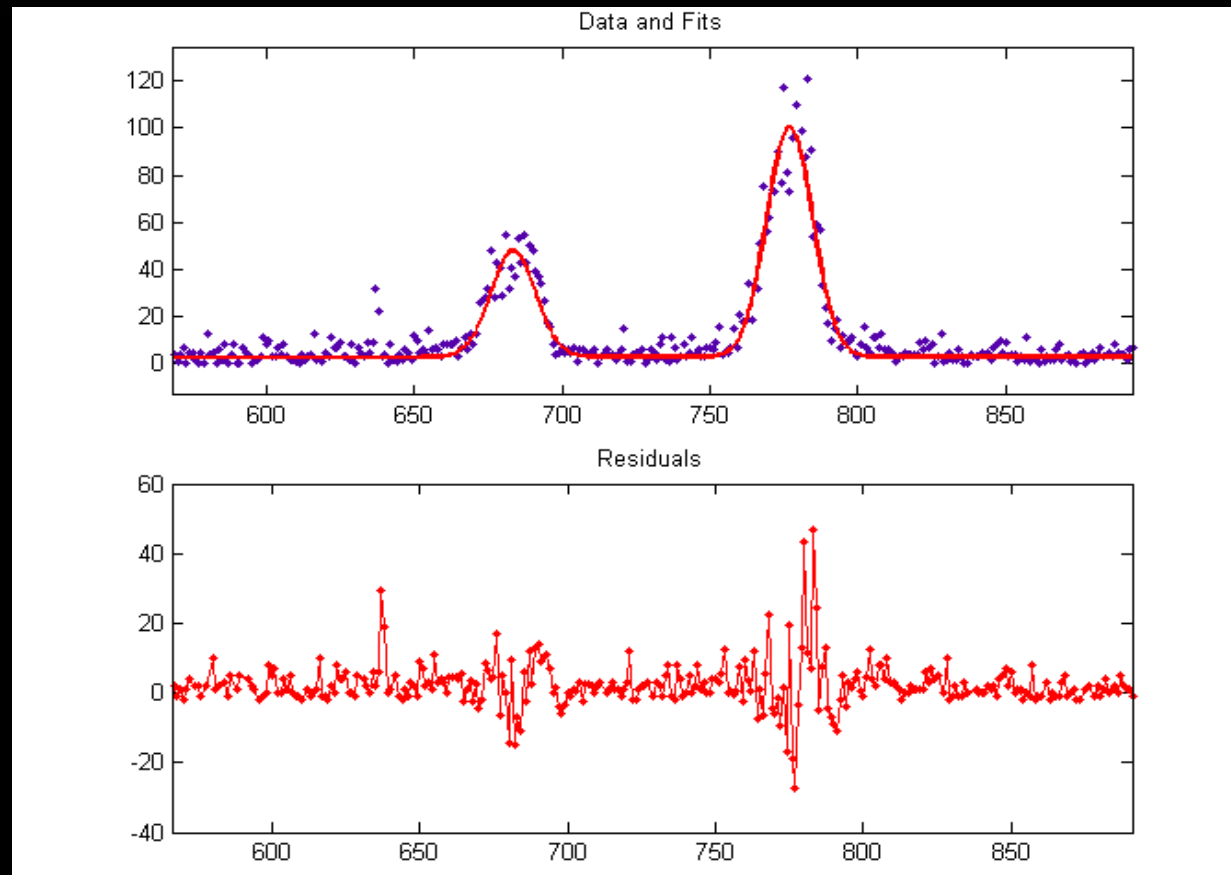


Our instrumental resolution is superior to that reported by Chantler.

We are currently investigating the extent to which we can extract/simulate sufficient information about our instrumental function and so correct our calibration data.



Measuring $1s_{1/2}-2p_{1/2,3/2}$ in Cr^{23+}



Work in progress (Toleme)

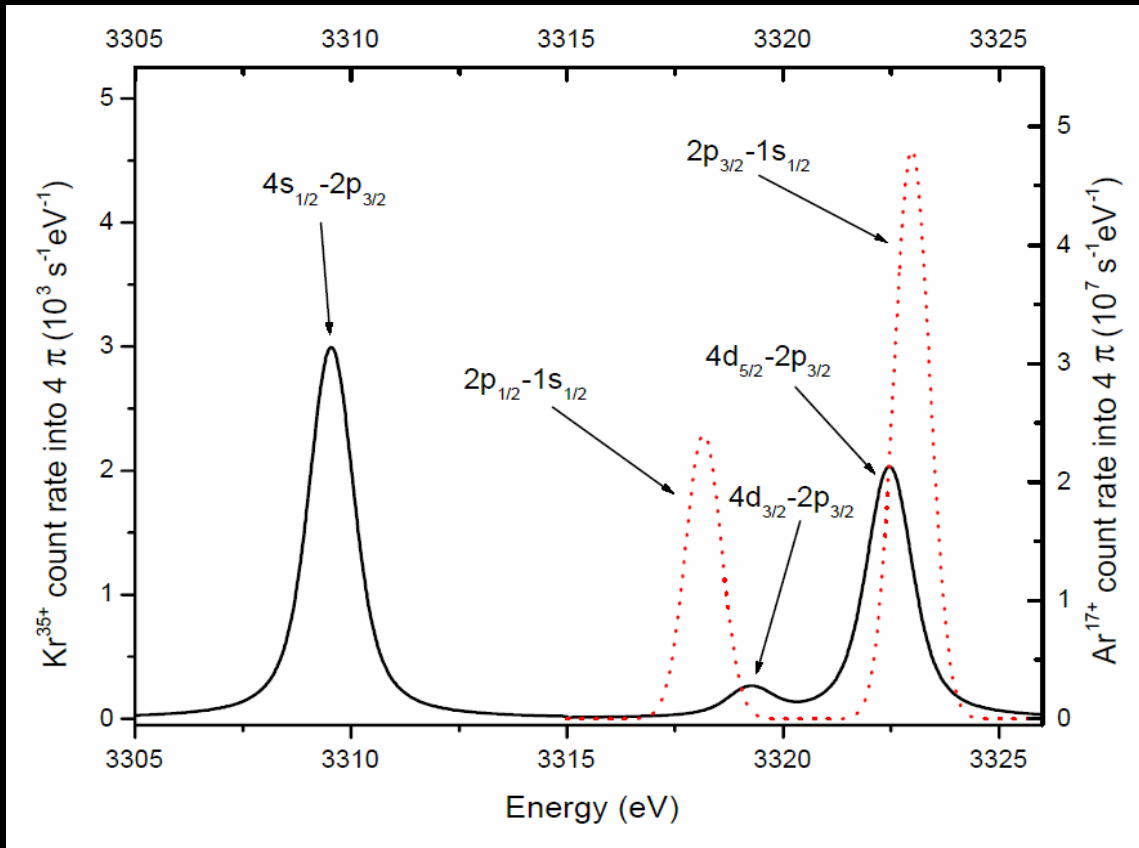


X-ray spectroscopy – intercomparison experiments

$$E(n, k, Z) = \left[1 + \frac{(Z\alpha)^2}{[n - k + (k^2 - (Z\alpha)^2)^{1/2}]^2} \right]^{-1/2} m_e c^2$$

Solutions to Dirac equation invariant under transformation

$$n \rightarrow an, k \rightarrow ak, Z \rightarrow aZ$$



Extract measurements of differences of QED and nuclear contributions.

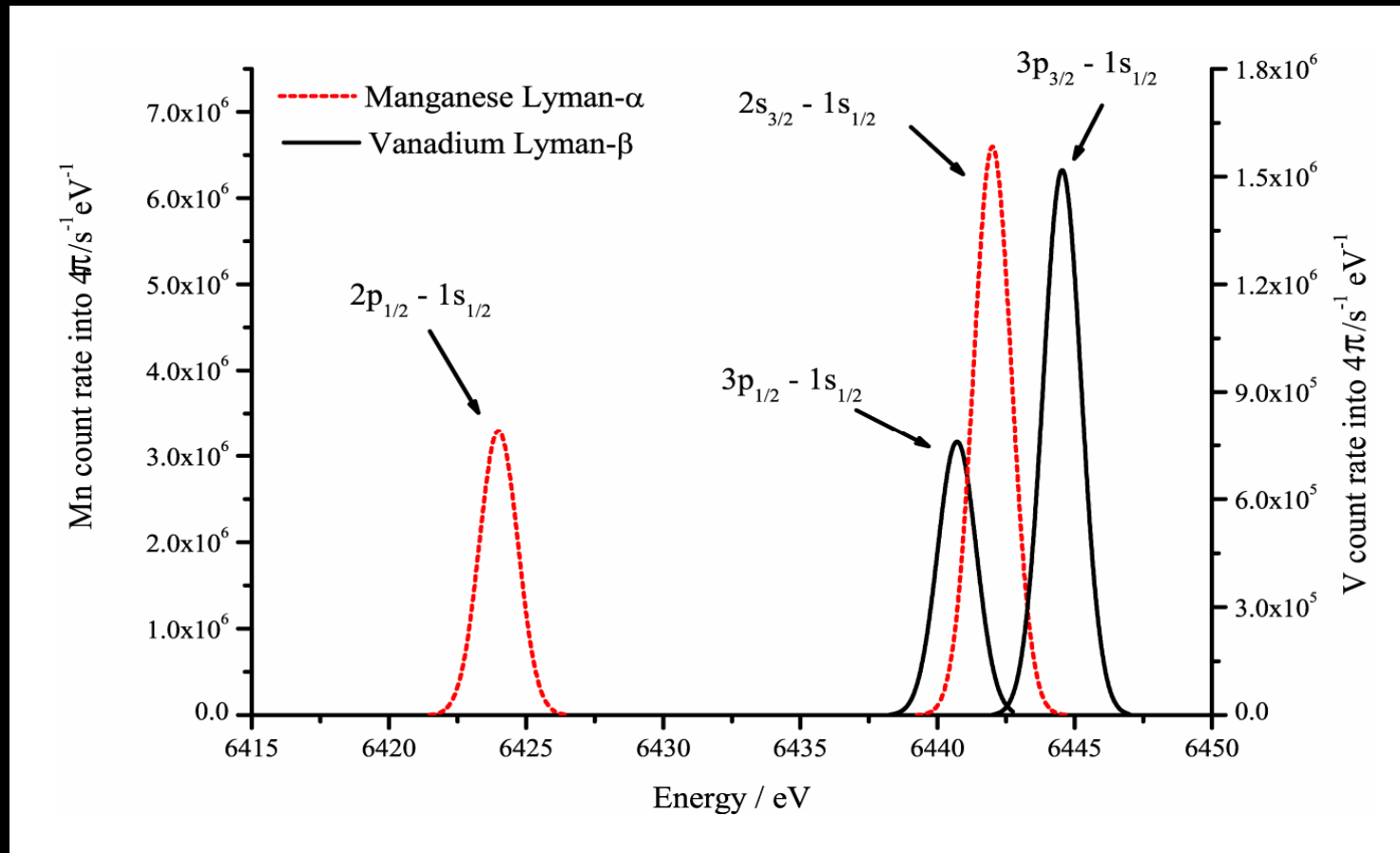
This may be achieved at x-ray wavelengths by observing different transitions in different hydrogen-like ions at different orders of diffraction – e.g. observe $\text{Ar}^{17+} 1s_{1/2} - 2p_{1/2,3/2}$ transitions and $\text{Kr}^{35+} 2p_{3/2} - 4s_{1/2}, 2p_{3/2} - 4d_{3/2,5/2}$ transitions

However systematic effects, such as refractive index changes make such attempts difficult



X-ray spectroscopy – intercomparison experiments

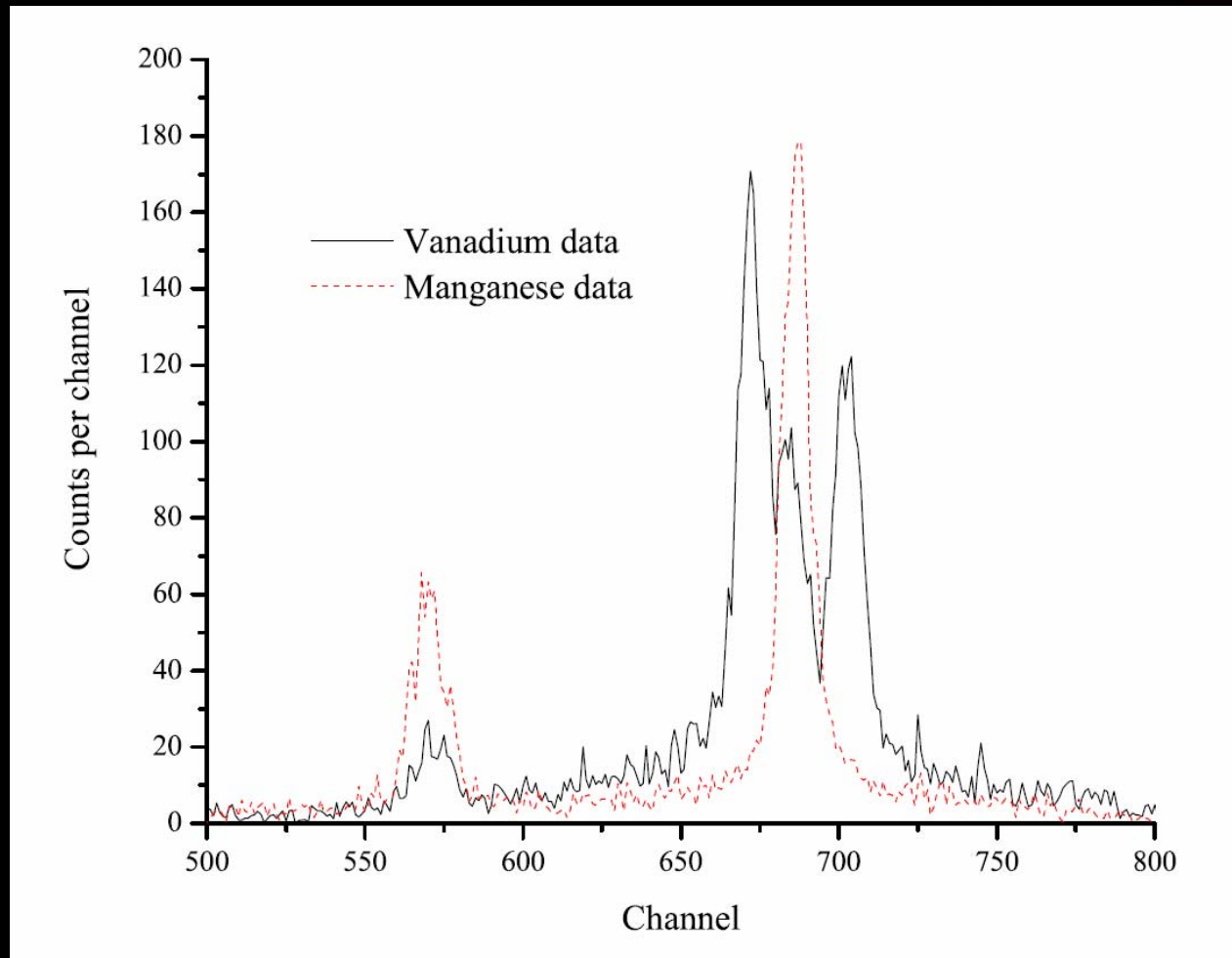
Instead find close lying transitions in different ions which may be observed in the same order.



e.g compare $1s_{1/2} - 3p_{1/2,3/2}$ transitions in V^{22+} with $1s_{1/2} - 2p_{1/2,3/2}$ transitions in Mn^{24+} . Difference of 2.8 eV between $1s_{1/2} - 3p_{3/2}$ and $1s_{1/2} - 2p_{1/2}$ is highly sensitive to difference in Lamb shifts (0.9 eV of this difference).



X-ray Intercomparison - results

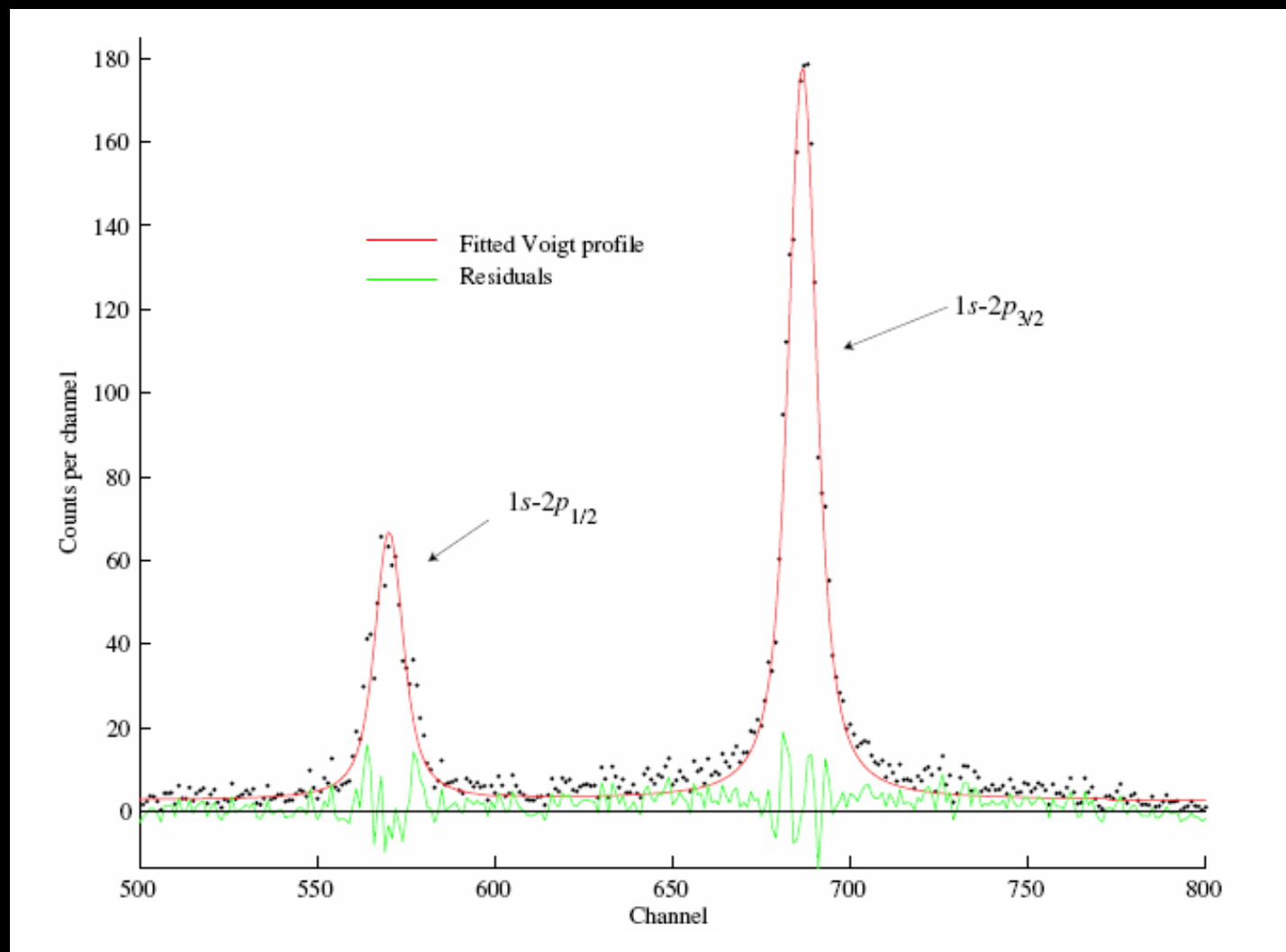


Should be possible to obtain a measurement accuracy equivalent to absolutely calibrated measurement of ~ 1 ppm accuracy with current apparatus.

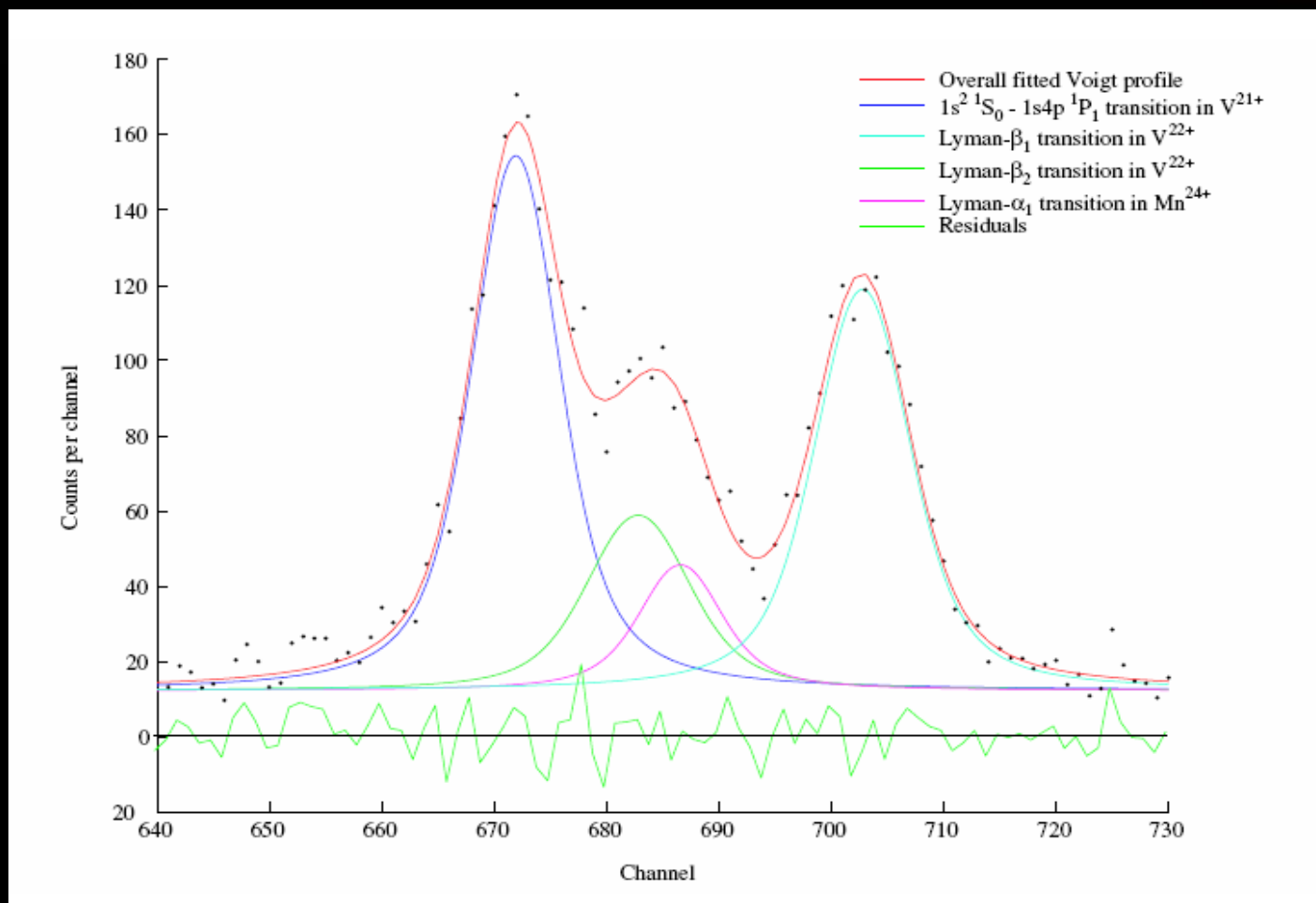
This would test calculations of the ground state Lamb shift at $\sim 0.1-0.3\%$ level



Intercomparison results – Mn²⁴⁺ data



Intercomparison results – V²²⁺ data



Transition blended with Helium-like Vanadium line (unavoidable) AND with Mn^{24+} contaminant – an unfortunate consequence of organometallic gas injection

NB: contamination is not long term and is only present in pre-injection chamber of gas injector.



Injection methods for EBIT

Requirements for new injection method for EBIT:

- ✦ Reliable
- ✦ Versatile – not limited to conductors
- ✦ Rapid switching between elements
- ✦ Low contamination
- ✦ Efficient (we really want to maximize our photon output)

Other recent approaches (both look promising):

Better MeVVA engineering (NIST):

Holland *et al.*, *Rev. Sci. Instrum.*, **76**, 073304 (2005)

Laser ion source – use a laser pulse rather than an electrical discharge to generate plasma (Heidelberg):

Trinczek *et al.*, *Nucl. Instr. Meth. B*, **251**, 289 (2006)



Estimating the Maximum Photon Output

Trap capacity, assuming all ions ionized to Hydrogenlike:

$$N \left(X^{(Z-1)+} \right) \approx \frac{4 \times 10^7 I_e (\text{mA})}{(Z-1)} \text{ ions}$$

Approx photon production rate, assuming tuned to maximum of excitation cross-section:

$$\Phi \approx \frac{4 \times 10^8 I_e^2 (\text{mA})}{Z^6} \text{ Lyman-}\alpha \text{ photons/sec}$$

Photon Output Rate Estimate

$N_e = \frac{I_e l}{e v_e}$; no. electrons in trap length; $N_i = \frac{N_e}{(Z-1)}$ full neutralized with H- ions

$l \sim 2 \text{ cm}$ $I_e = 10^{-3} I_e (\text{mA})$

$e \sim 1.6 \times 10^{-19} \text{ C}$; $v_e (\text{cm s}^{-1}) = 100 \sqrt{\frac{2e \Phi (\text{eV})}{m_e}}$

$m_e \sim 9.11 \times 10^{-31} \text{ kg}$

Max X-section approx. $11 \times 3 \times Z^2 (\text{eV}) = E (\text{eV})$

$v_e = 3.6 \times 10^8 Z \text{ cm s}^{-1}$

$N_e = \frac{I_e (\text{mA})}{1.7 \times 10^{11} Z e}$

$Z \sim Z-1$

so: $N_i \sim \frac{3.7 \times 10^7 I_e (\text{mA})}{Z^2}$; N_i ions in full trap

excitation rate $R = \frac{j_e}{e} \sigma_{ee}$ $j_e = \frac{I_e (\text{mA})}{1000 \pi r^2}$; $r_e \sim 35 \times 10^{-4} \text{ cm}$

so $j_e \sim 26 I_e (\text{mA}) \text{ A/cm}^2$

so $R \sim 1.6 \times 10^{18} I_e (\text{mA}) \cdot \frac{6 \times 10^{-18}}{Z^0} \approx \frac{10 I_e}{Z^0}$

Max $\Phi = R N_i$

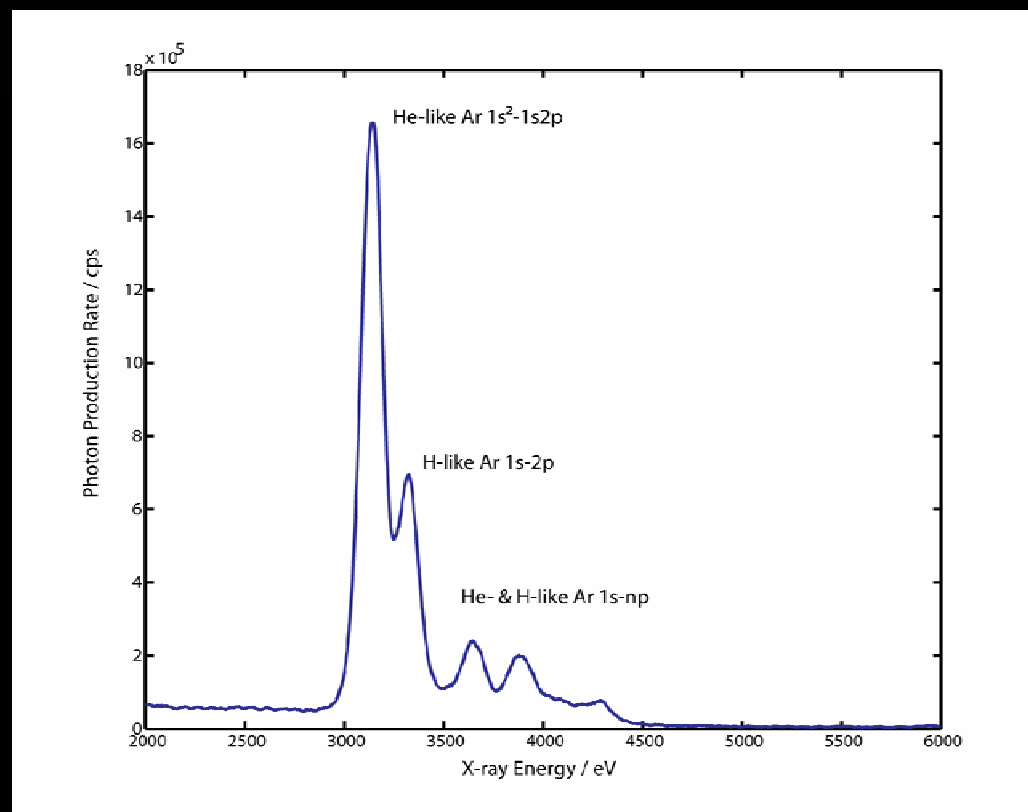
so: $\Phi = 3.7 \times 10^8 \frac{I_e^2}{Z^6}$

上海张江艾西益
地址: 浦东国际机场
碧波路635号
祖冲之路1559号创意大厦

SHANGHAI ZHANGJIANG AIXIYI



Photon Output – Argon example



Argon injected into EBIT running with an 18 keV¹, 140 mA electron beam.

¹ Somewhat above the peak cross section energy at ~10 keV

Measured Lyman- α Photon Yield:

$\text{Ar}^{17+} \sim 0.7 \times 10^7$ photons/sec

$\text{Ar}^{16+} \sim 2.1 \times 10^7$ photons/sec

Correcting for larger Ar^{16+} cross section (approx 2xH-like) H-H-like equivalent output rate $\sim 1.75 \times 10^7$ photons/sec

Calculated estimate $\sim 5 \times 10^7$ photons/sec (corrected for higher beam energy)



MIVOC and MeVVA Photon Count Rates

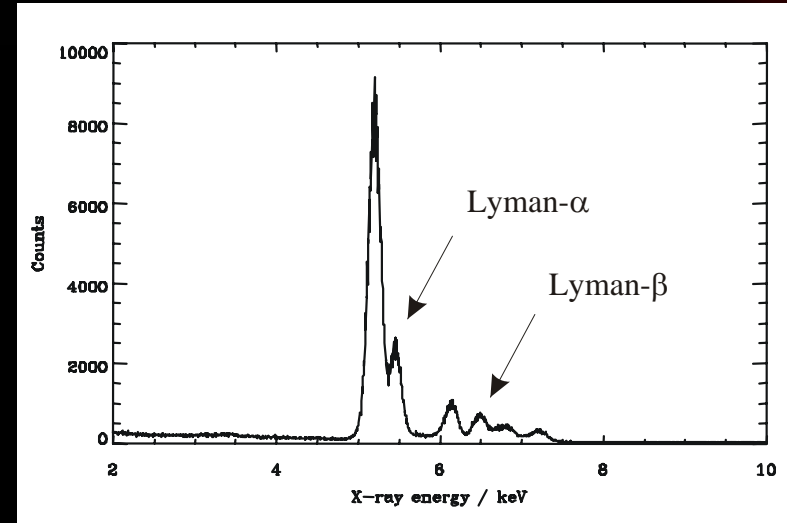
V^{22+} , 15 keV, 100 mA beam
Predicted max count rate
 1.4×10^7 photons/sec

MIVOC results for V^{22+} Lyman- α using
Vanadocene $(C_5H_5)_2V$:
 3.0×10^6 photons/sec
(H-like equivalent rate)

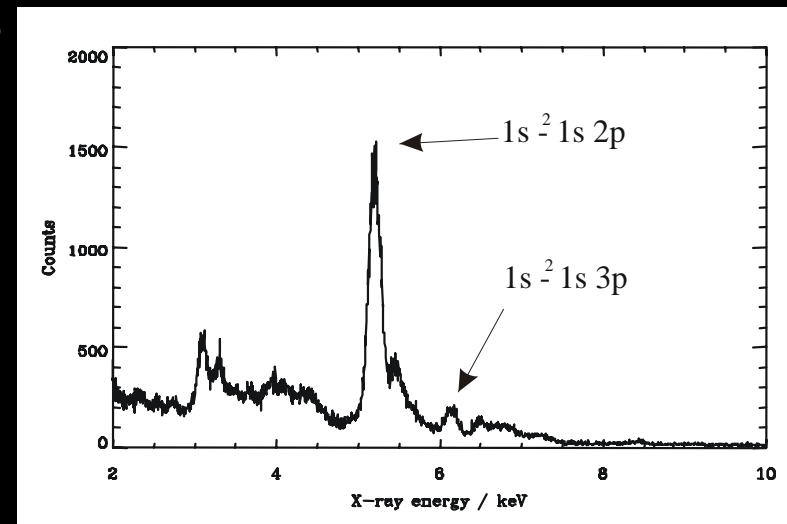
MeVVA results for V^{22+} Lyman- α : 1.1×10^6
photons/sec
(H-like equivalent rate)

(Note contamination – performance was erratic and
showed large shot-to-shot fluctuations)

Neither close to maximum or as
good as that obtained with gas
injection of Ar



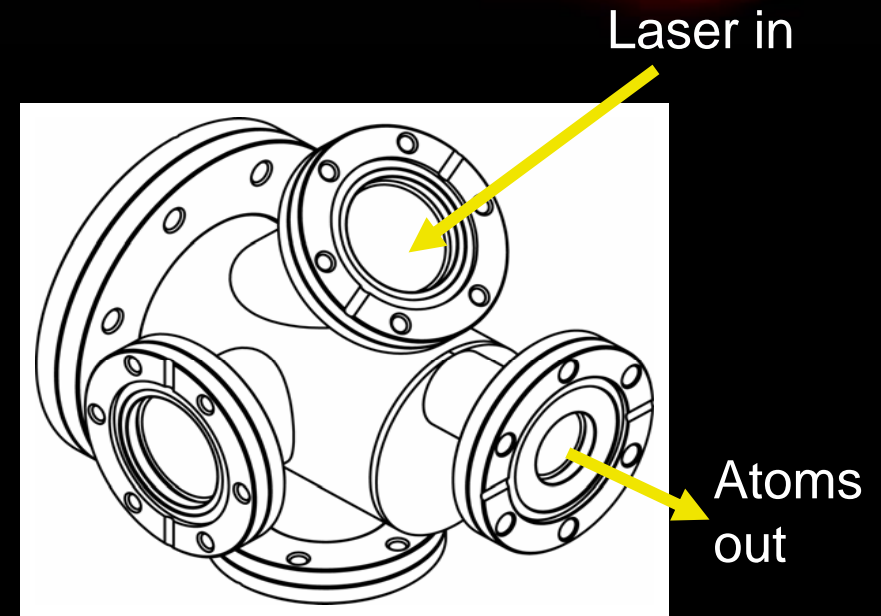
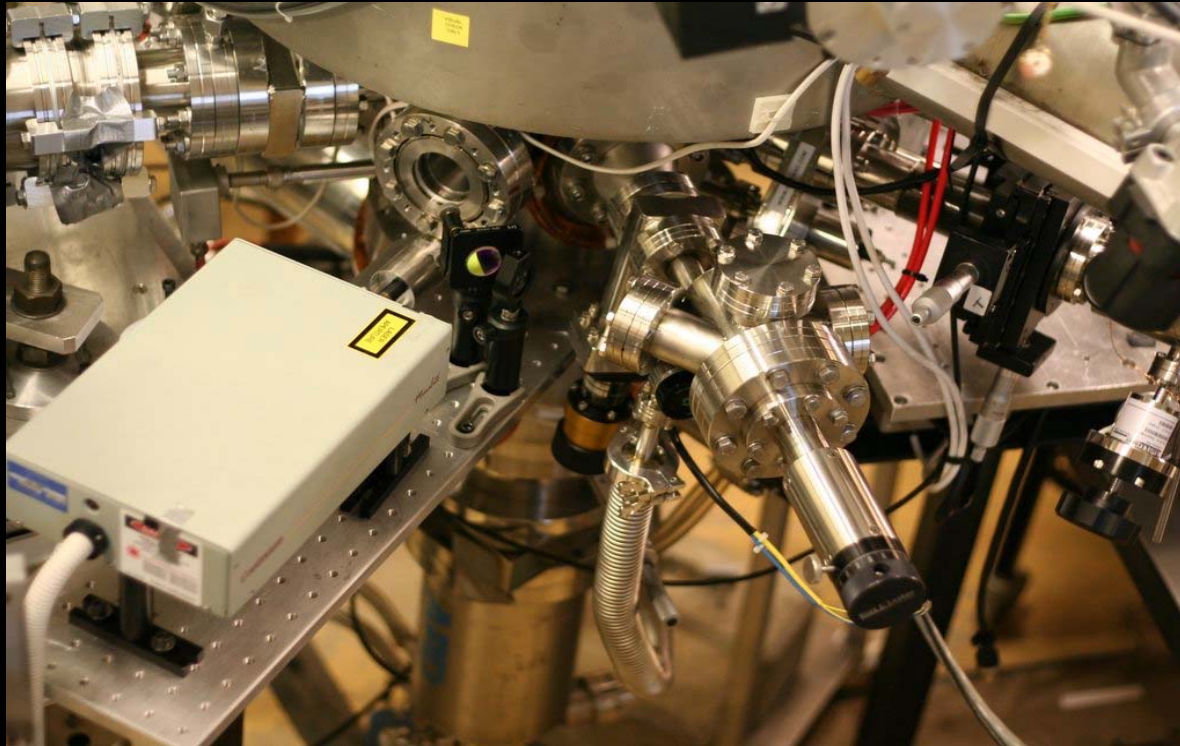
MIVOC – Organometallic vapour injection



MeVVA injection



Laser Ablation of Neutral Atoms



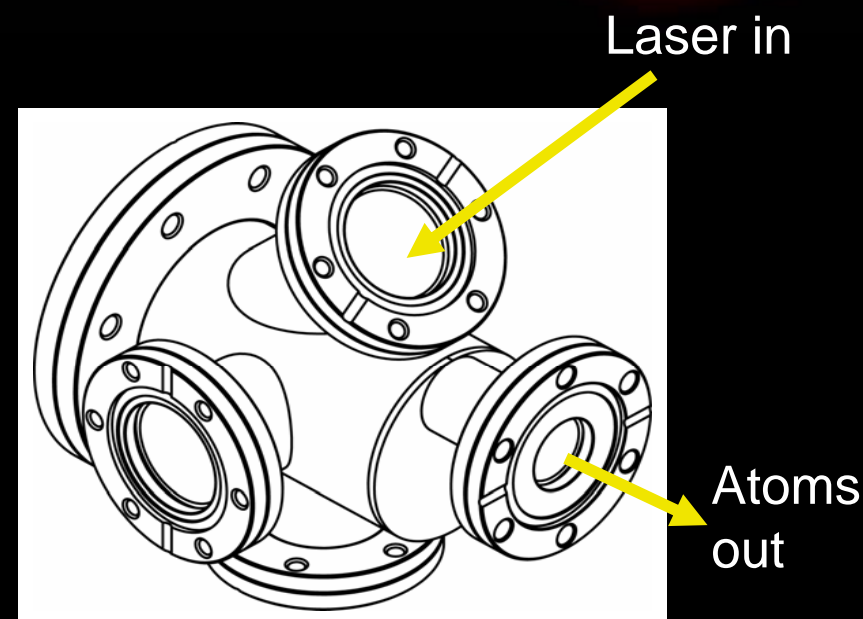
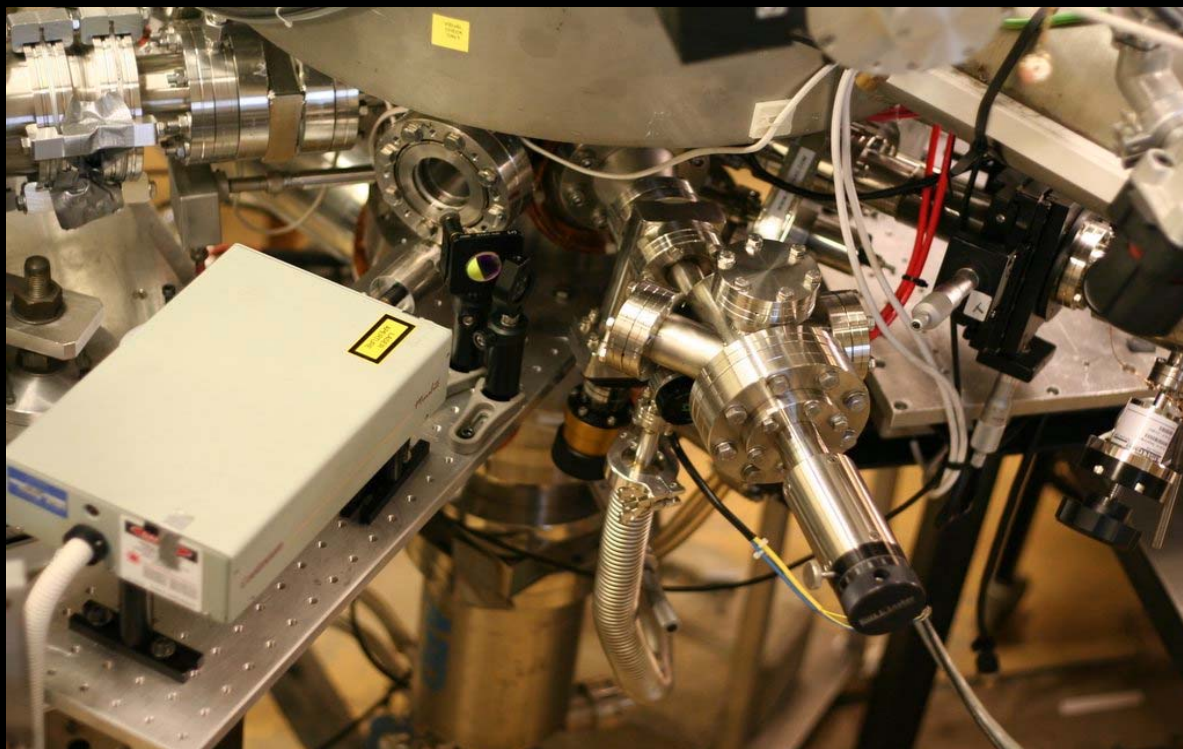
✶ Atoms injected radially into EBIT via observation port opposite to the gas injector

✶ Laser source: Frequency doubled Coherent Minilight Nd:YAG laser, 12 mJ/pulse, 6 ns pulse duration, 10 hz maximum repetition rate, focussed to spot ~0.7 mm diameter (i.e. modest and inexpensive)

- Much lower intensity to ablate atoms than required to generate plasma for ion injection
- Estimate 10^{13} - 10^{15} atoms/pulse depending on element.



Laser Ablation of Neutral Atoms



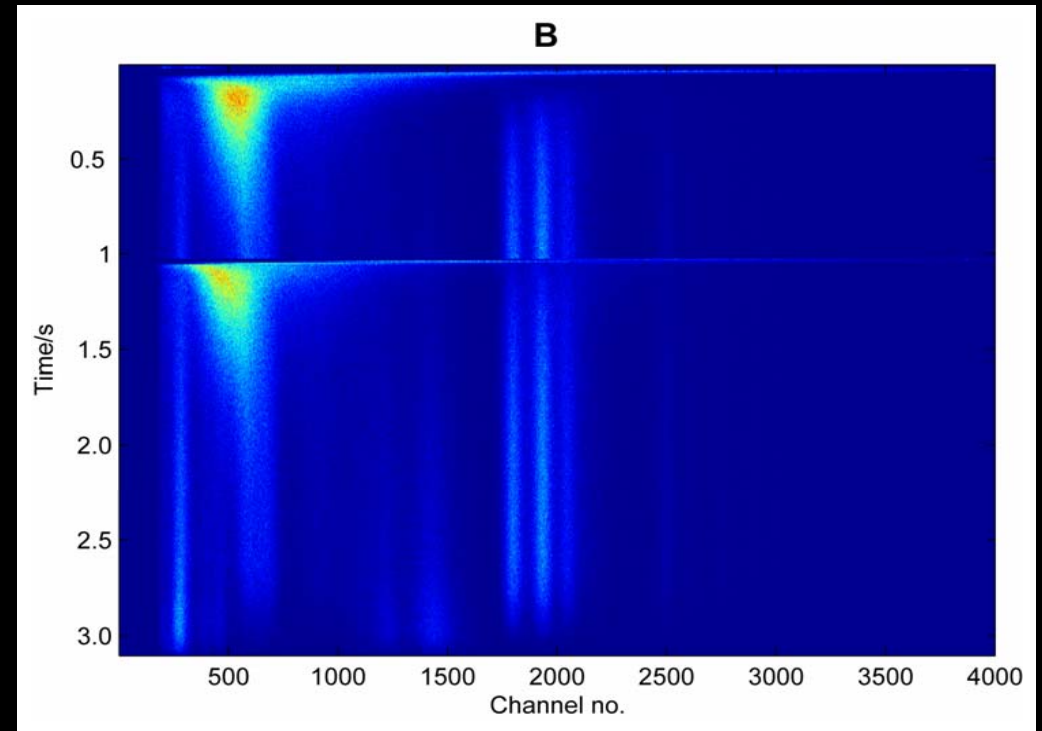
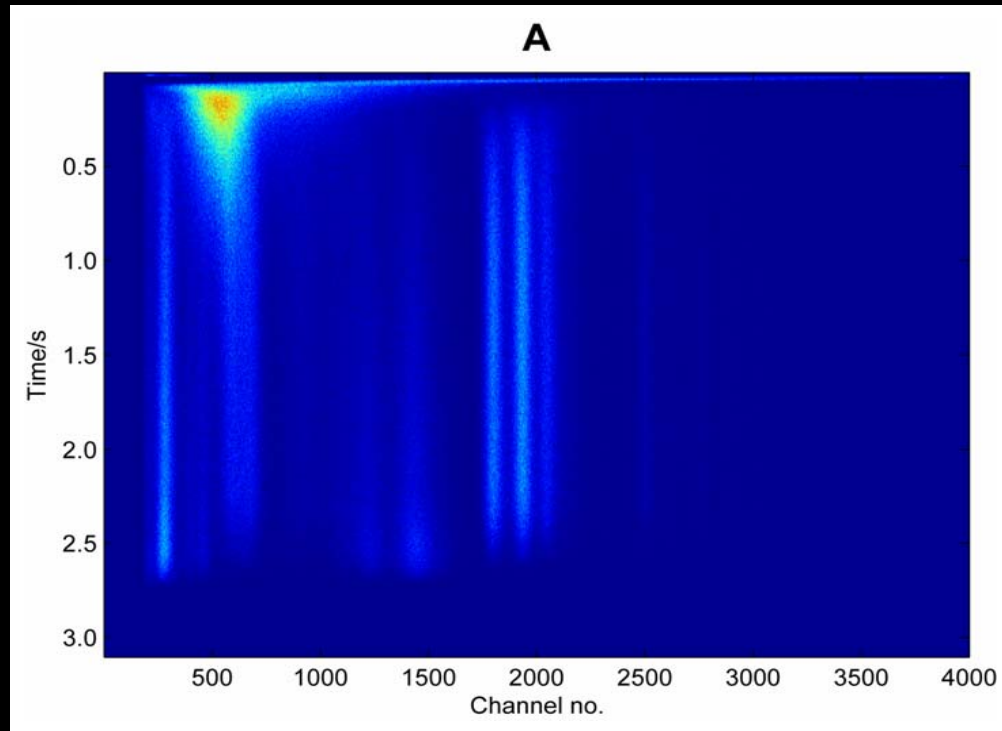
Recipe: Run EBIT, fire laser at target, get ions. Change element by rotating target wheel (takes seconds). Current design holds up to six different targets.



Old Recipe (MEVVA): Run EBIT, carefully synchronize ion beam trigger sequence, sometimes get some ions + contamination. Change element by breaking MEVVA vacuum and replacing cathode (takes hours).



Laser Ablation – Results

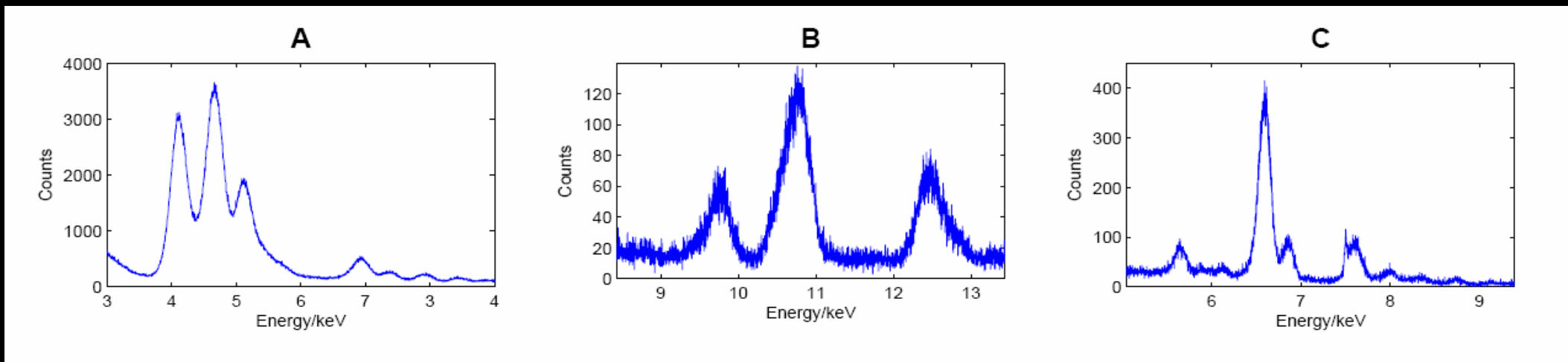


Laser ablated injection of Tin, forming Neonlike Sn^{40+}

A = 1 laser pulse. B = 2 laser pulses



Laser Ablation – Results



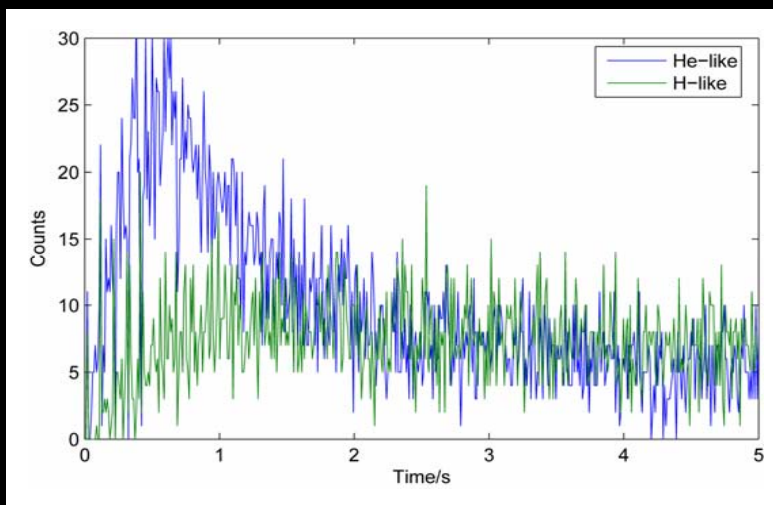
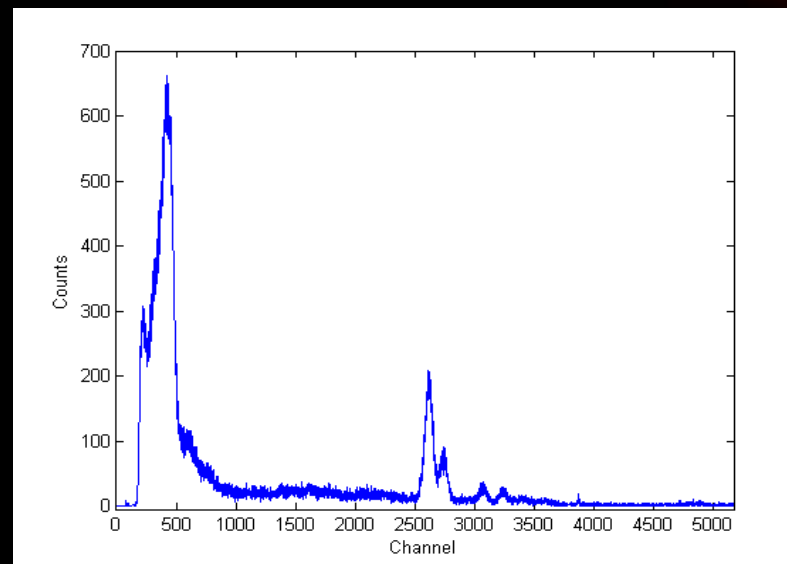
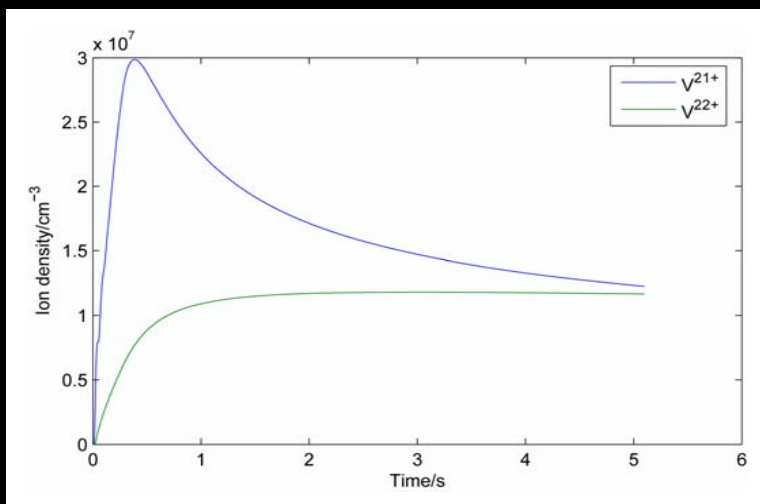
Injection of A: Tin, B: Lead, C: Stainless Steel



Have successfully injected every element tried – Vanadium, Manganese, Iron, Copper, Nickel, Tin, Lead



Laser Ablation – Results

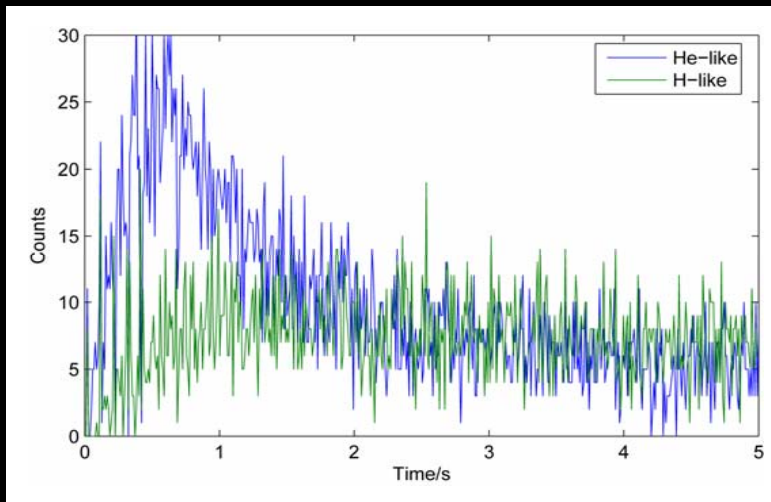
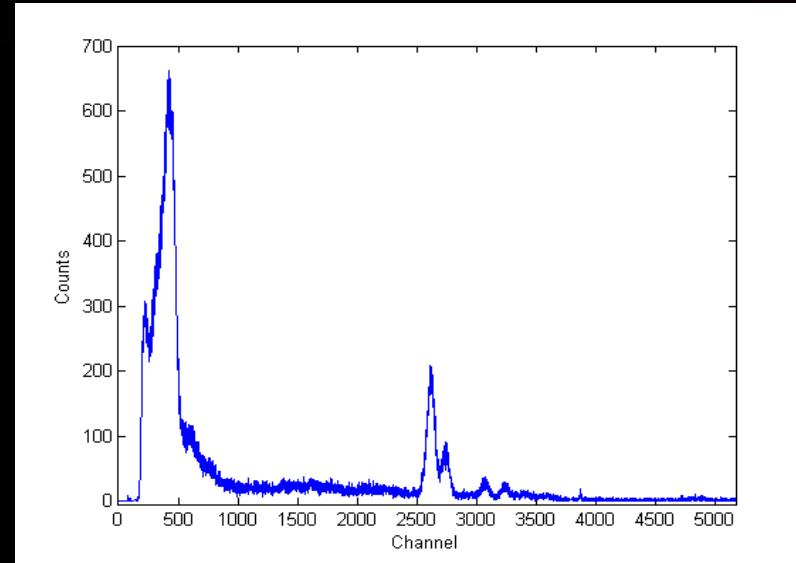
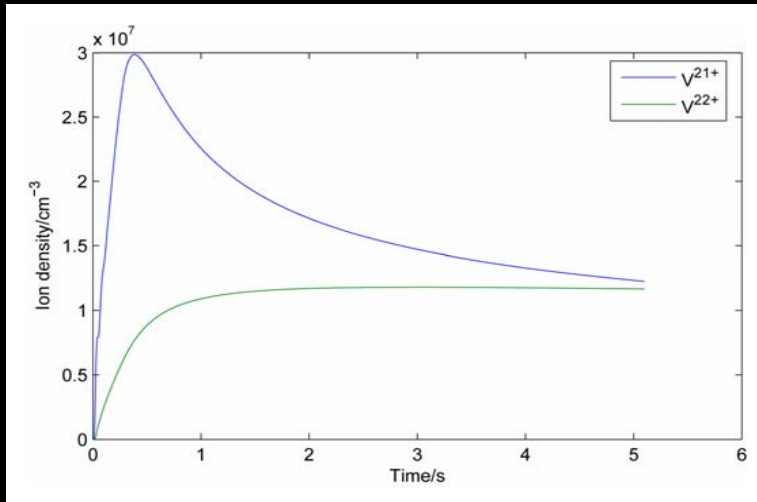


Injection of Vanadium – successful production of hydrogenlike and heliumlike ions consistent with simulation.

Lyman- α count rate 1.3×10^6 cps (15keV, 100mA beam), similar to MeVVA, somewhat less than MIVOC and theoretical limit.



Laser Ablation – Results







Technique needs to be carefully optimized if maximum performance is to be realised.

It is not yet clear whether it will outperform MeVVA or MIVOC. Pip Pip!



Dabbling in EBIT kinetics

Careful experimentation requires that all aspects are as well understood as possible. To this end, and with respect to our spectroscopy experiments we have been asking ourselves a number of questions:

-  What is the magnitude of Doppler shifts across the ion cloud profile?
-  To what extent does the ion radiative distribution reflect the actual ion distribution?
-  What should we do to improve the quality of our EBIT modeling and can this improve our results?
-  Many spectroscopic measurements are limited by Doppler broadening. Can we make the ions colder without sacrificing too much flux?



Modelling – electron beam transport



Model of Oxford EBIT constructed using commercial package – OPERA 3D from Vector Fields [1]



Solve for electrostatic and magnetostatic potentials by finite element method
(Galerkin weighed residual method)



Solve electron beam transport problem including space charge by an iterated self-consistent method

$$V_{n+1}^{tot} = V_n^{tot} + \alpha V_n^{beam}$$



Monte Carlo method employed to include thermal effects in trajectory simulation – intention is to compare results against the predictions of Hermann theory

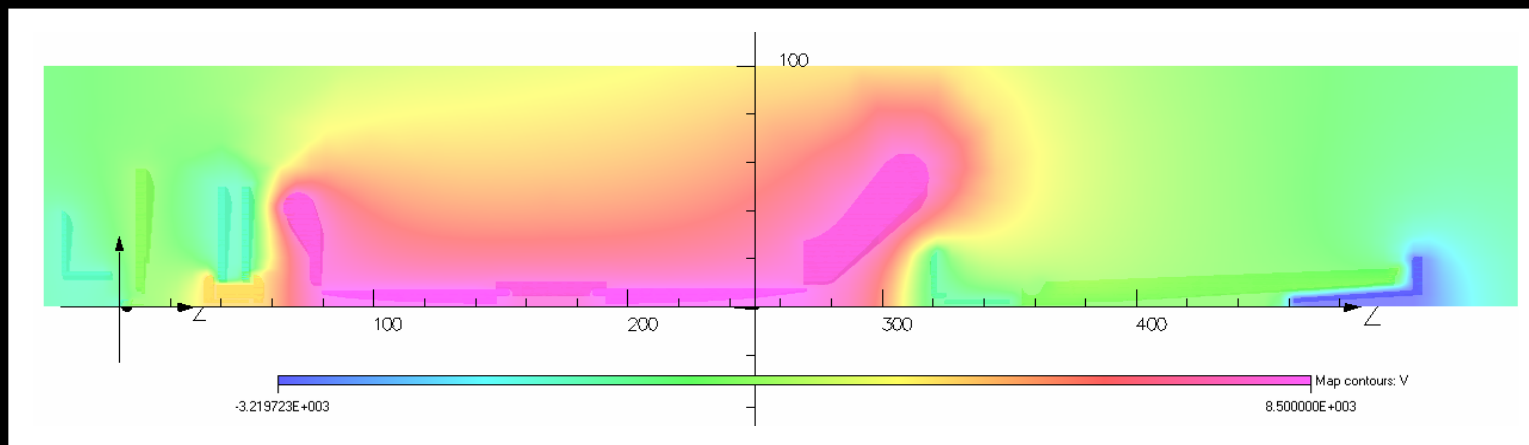
[1] <http://www.vectorfields.co.uk>



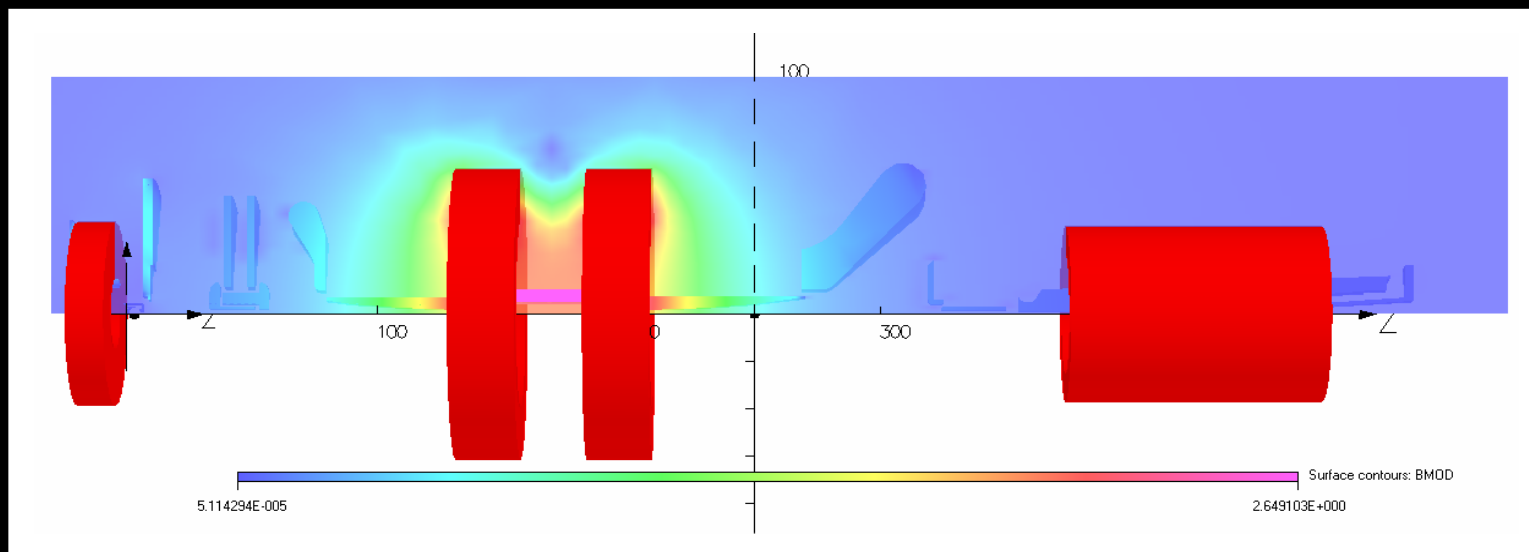
Results – no electron beam




Electrostatic potential




Magnitude of B-field




Modelling electron trajectories




Given the crucial role played by the initial thermal distribution of the electrons as predicted by Hermann theory wish to construct a model which includes thermal effects




Monte Carlo method – generate a set of trajectories, Boltzmann distributed in velocity space and distributed across cathode surface according to result of a Child's Law simulation
(ideally the explicit use of Child's Law should be unnecessary, however it is not possible at present to mesh the gun region with sufficient resolution to accurately model the expected virtual cathode)



Find a self-consistent solution for these trajectories
(ideally a new set of trajectories should be generated for each iteration, however, this has not been implemented as of the present time)



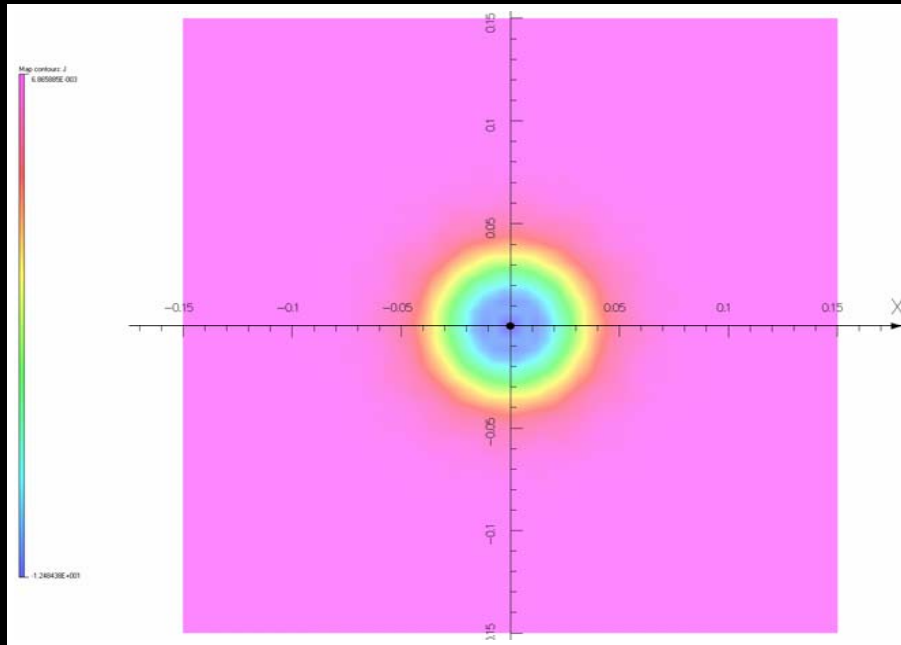
Make comparisons against Hermann theory
(e.g. compare beam size as a function of magnetic field at the cathode surface)


$$r_H = r_B \left\{ \frac{1}{2} + \frac{1}{2} \left[1 + 4 \left(\frac{8m_e k T_c r_c^2}{e^2 B^2 r_B^4} + \frac{B_c^2 r_c^4}{B^2 r_B^4} \right) \right]^{1/2} \right\}^{1/2}$$



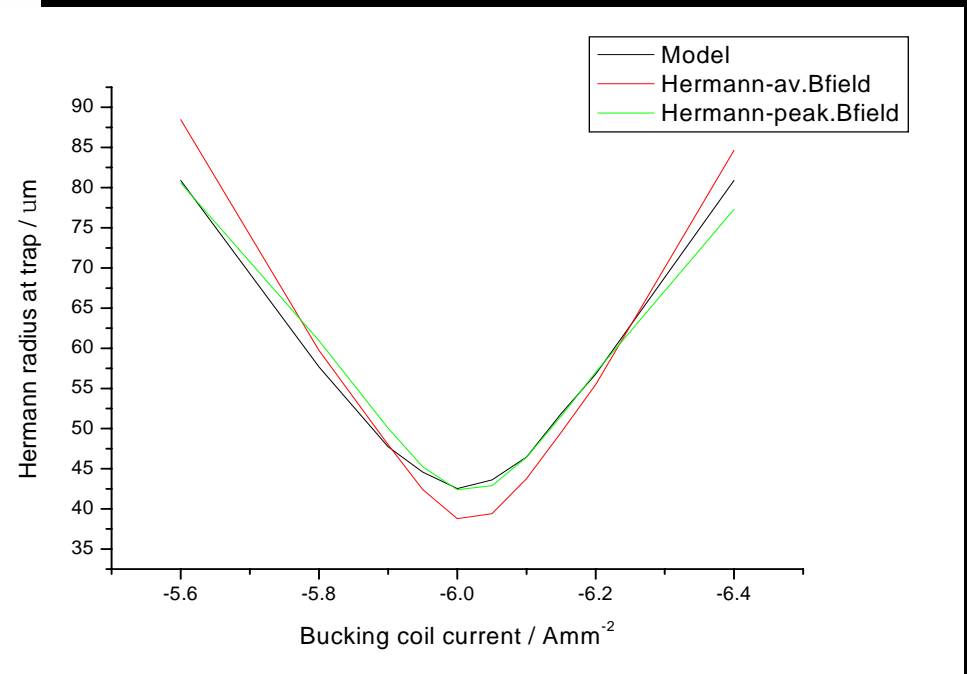
Results – electron beam transport

The results of the simulation appears to be in reasonable agreement with Hermann theory



Electron beam current density at trap centre

Comparison of radius of electron beam with predictions of Hermann theory

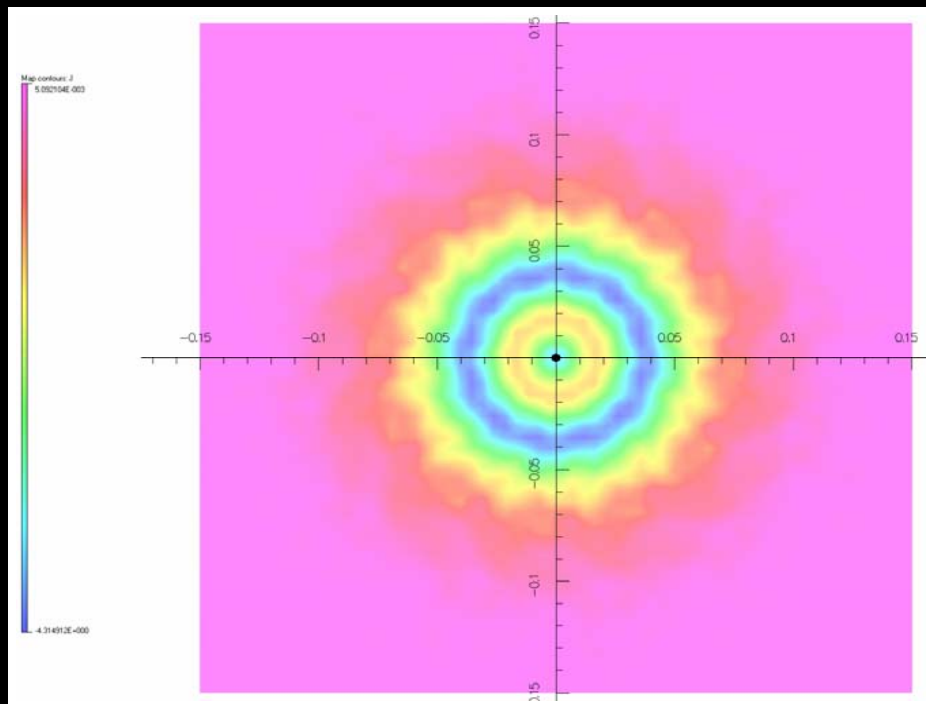


Simulated: 8.0 keV, 50 mA beam



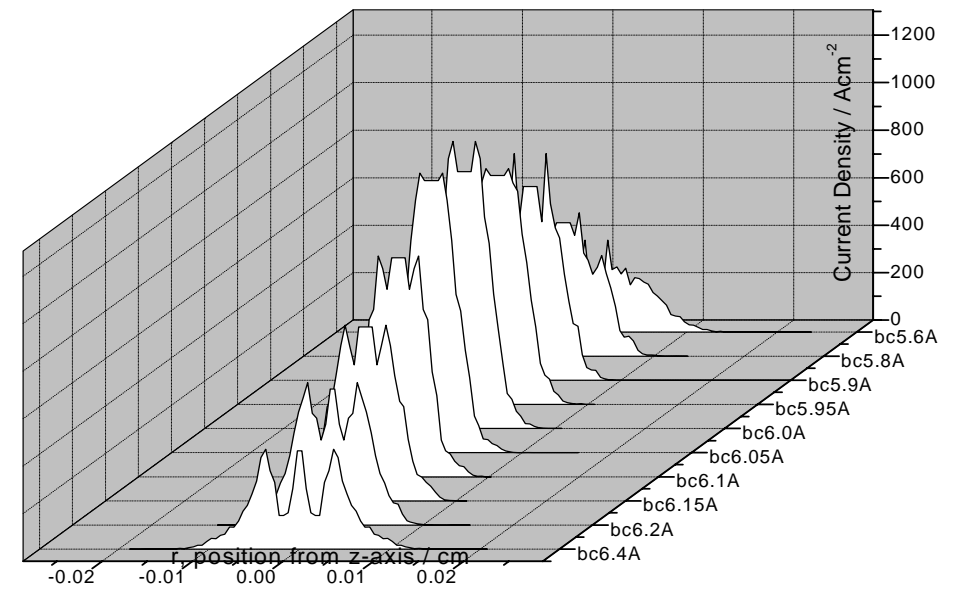
Results – electron beam transport

However, examining deeper we see that there is a qualitative modification of the electron beam profile from a centrally peaked, quasi-Gaussian to a halo beam for beam trajectories which pass through a sign reversal of the z-component of the magnetic field B_z



Electron beam current density at trap centre – a distinct halo with a central spike is formed

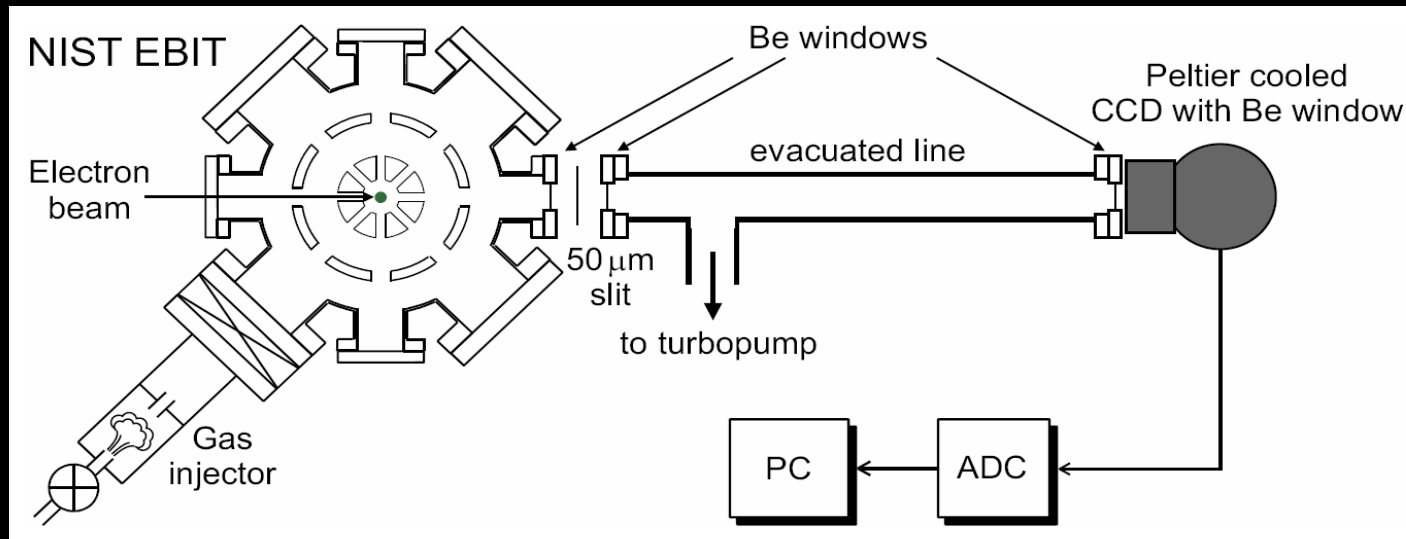
Electron beam profile for a range of bucking coil current densities (and so magnetic fields at the cathode surface)



Experimental evidence

Evidence from experiments on NIST EBIT suggest behaviour irreconcilable with Hermann theory [1] – asymmetric relationship between field at electron gun cathode (as controlled by changing

Measure electron beam – ion cloud overlap profile in Cartesian projection by x-ray pinhole (or rather slit) method

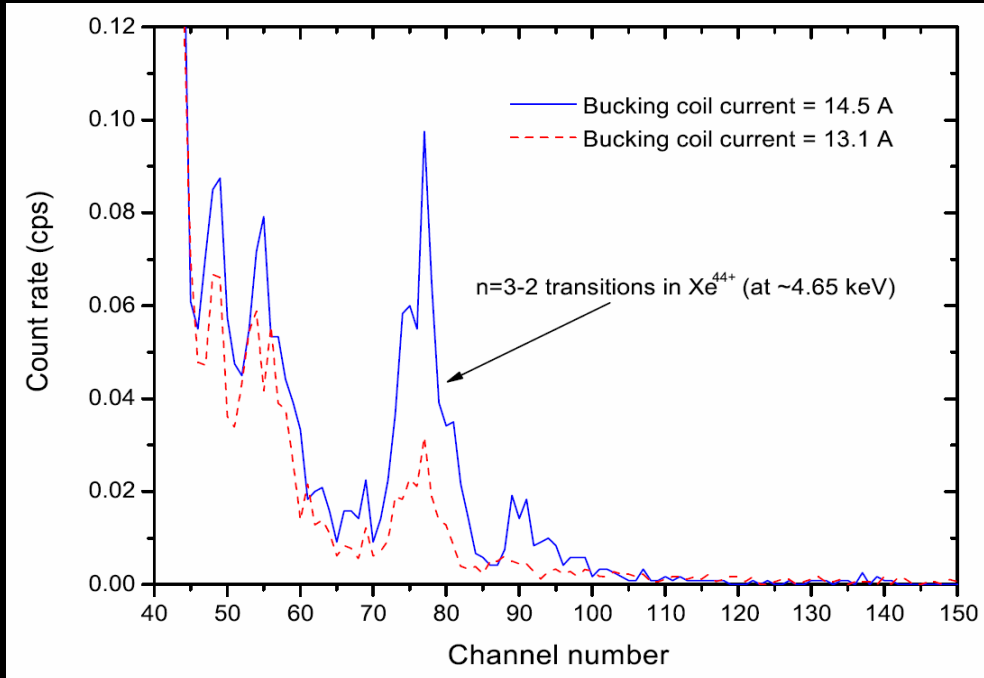


[1] E. Takács, private communication – discovered independently of and prior to this simulation work

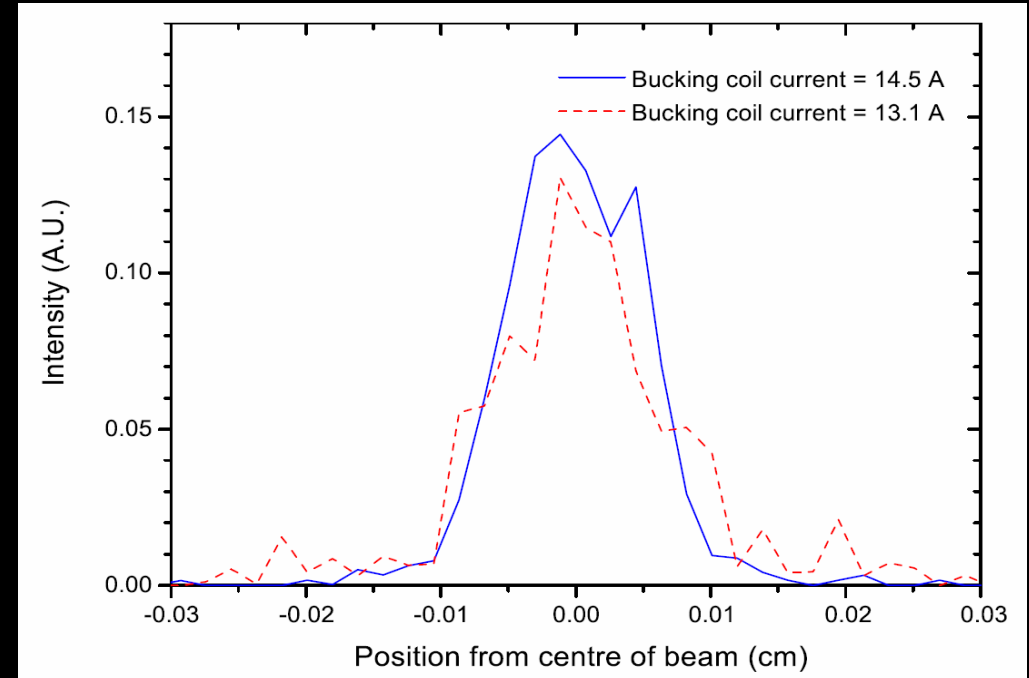


Experimental evidence – results

EDS spectrum generated by CCD



Measured radiative profiles

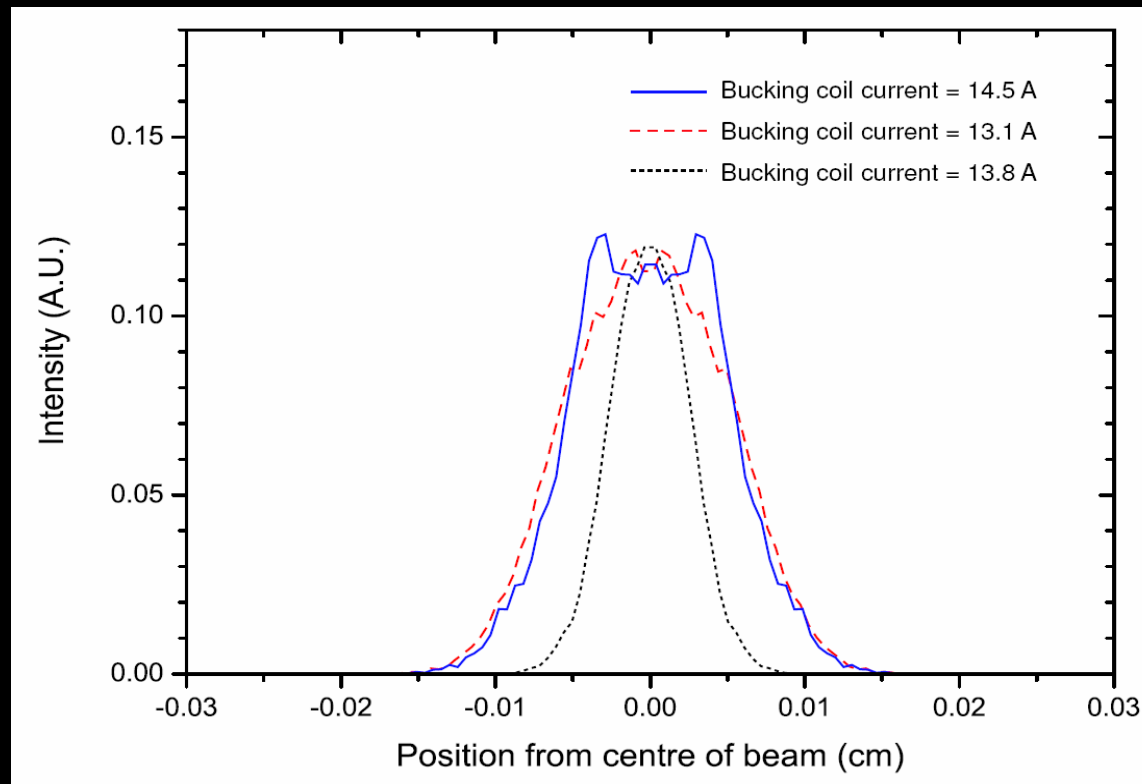


The difference in x-ray count rate is clear, despite there being no corresponding obvious change in the profile.



Experimental evidence – results II

We want to get density profiles as a function of radial coordinate. Unfortunately, the Cartesian projection of the radiative profile is not a particularly sensitive, unambiguous means of measuring this...



Nevertheless, the difference in photon flux is very clear and should be explained. Given that we suspect a change in our electron beam profile we should look to the relationship between this and the ion cloud profile as a possible explanation.



Ion cloud distribution

In cylindrical coordinates (ρ, ϕ, z) the trapping potential, including the contribution due to the magnetic field can be written as

$$V_{\text{effective}}(\rho, \phi, z, \dot{\phi}) = V(\rho, z) + \frac{qeB^2}{8m_i} \rho^2 + \frac{L_i^2}{2m_i qe \rho^2}$$
$$L_i = m_i \rho_i^2 \left(\dot{\phi}_1 + \frac{qeB}{2m_i} \right)$$

Assuming that equilibrium is achieved the phase space distribution is

$$f(\mathbf{r}, \mathbf{v}) d^3 \mathbf{r} d^3 \mathbf{v} = n_0 \exp\left(-\frac{m_i v^2}{2kT}\right) \exp\left(-\frac{qV(\mathbf{r}, \mathbf{v})}{kT}\right) d^3 \mathbf{r} d^3 \mathbf{v}$$

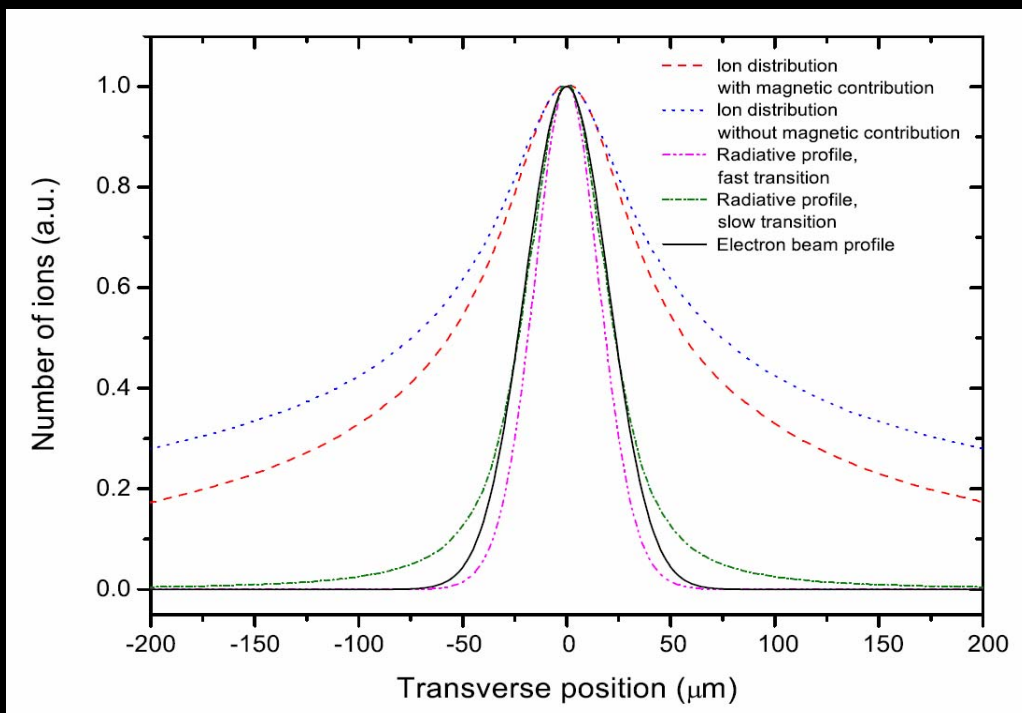
It's not clear whether we should use $V(\rho, z)$ or $V_{\text{effective}}$ for $V(\mathbf{r}, \mathbf{v})$. Complete kinetic (collisional) equilibrium implies the former given that the magnetic field does no work.

However EBIT is not necessarily in full equilibrium. So let's try a simulation and look at the results

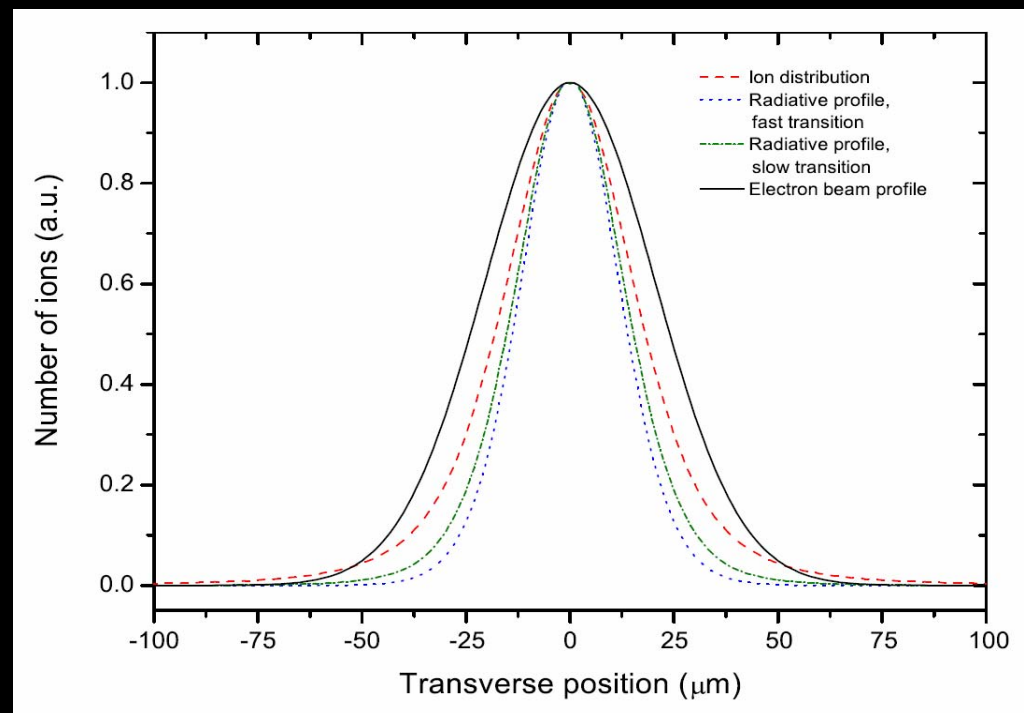


Ion Cloud Distribution vs. Radiative Distribution

N^{6+} at $T=100$ eV in 1.5 keV, 30 mA beam



Xe^{44+} at $T=500$ eV in 8.0 keV, 150 mA beam

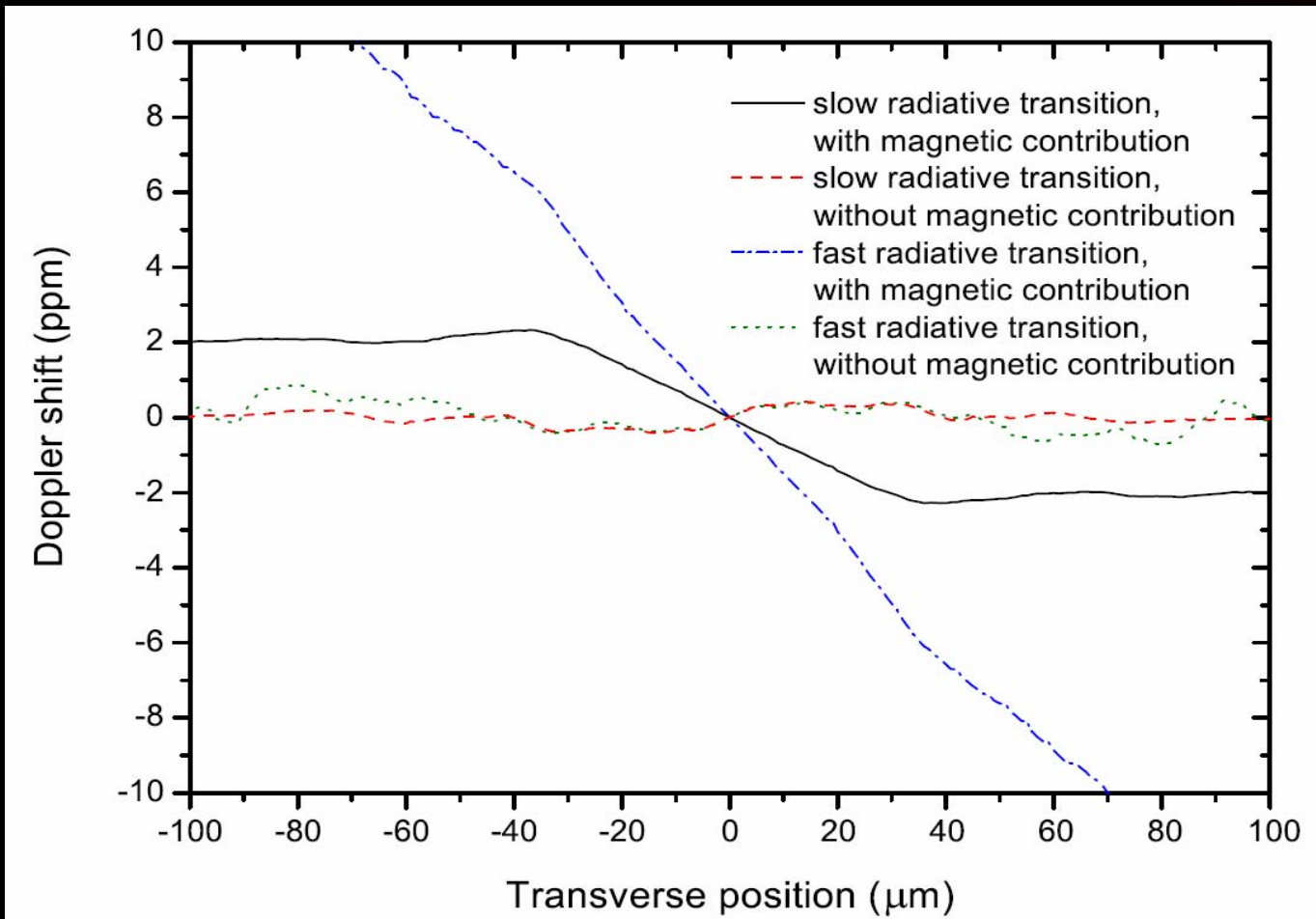


Effect of magnetic contribution to ion confinement on ion distribution can be quite significant

Effect of magnetic contribution to ion confinement on the shape of the radiative profile is negligible



Doppler shifts



N^{6+} at $T=100$ eV in 1.5 keV, 30 mA beam, averaged for a $20\mu\text{m}$ slit width

Whilst the overall Doppler shift of the ion cloud is zero* the effect of the magnetic field is a spatially dependent Doppler shift across the ion cloud profile. This can potentially be used to examine the magnetic contribution to ion confinement.

*excluding negligible second order Doppler shift and Doppler beaming effects)



Forced Evaporative Cooling

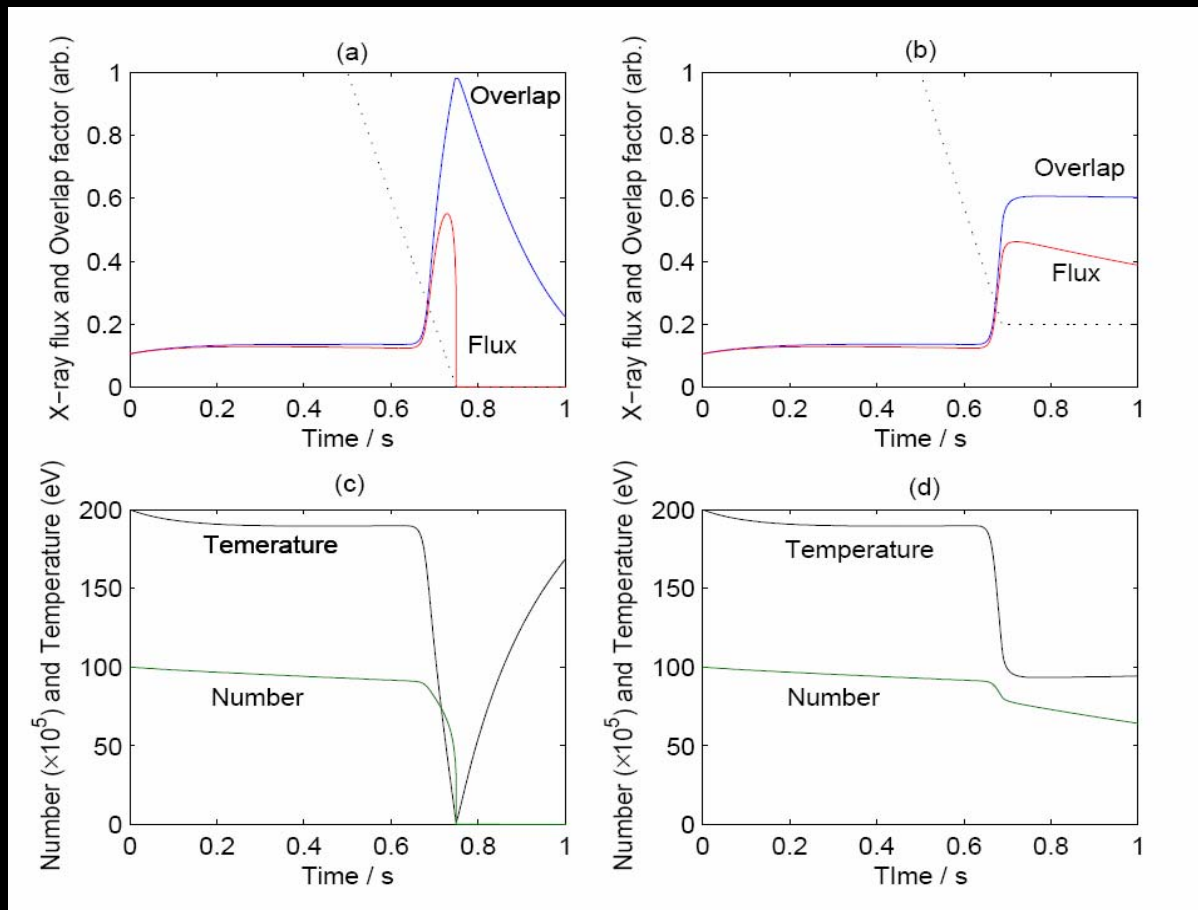
Many spectroscopic experiments on EBIT limited by Doppler broadening. Furthermore, hot ions can exhibit a very poor overlap with the ion cloud.

Can we do better?

Cooling ion cloud by changing the depth of the axial trap as a function of time – analogous to evaporative cooling technique of cold atom formation.

Original idea: Currell *et al.*, RIKEN Review, **31**, 52-55 (2000)

Related idea – cooling of extracted ion beam: Marrs, NIMB, **149**, 182 (1999)



Simulation of evaporative cooling from EBIT.

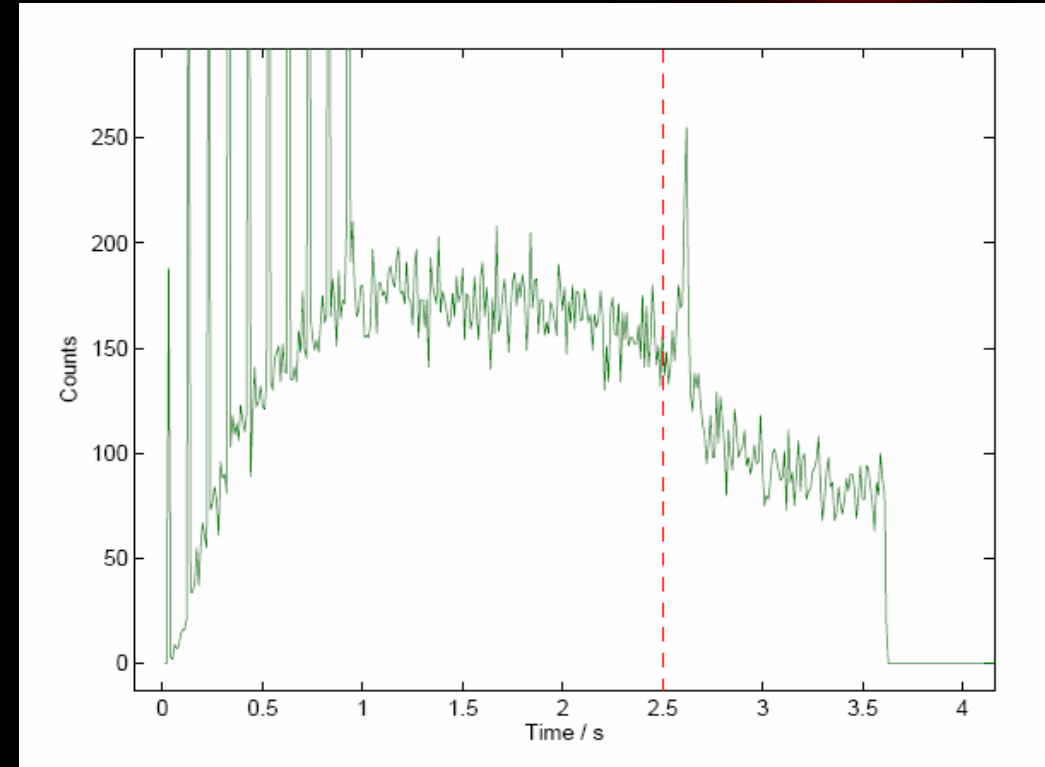
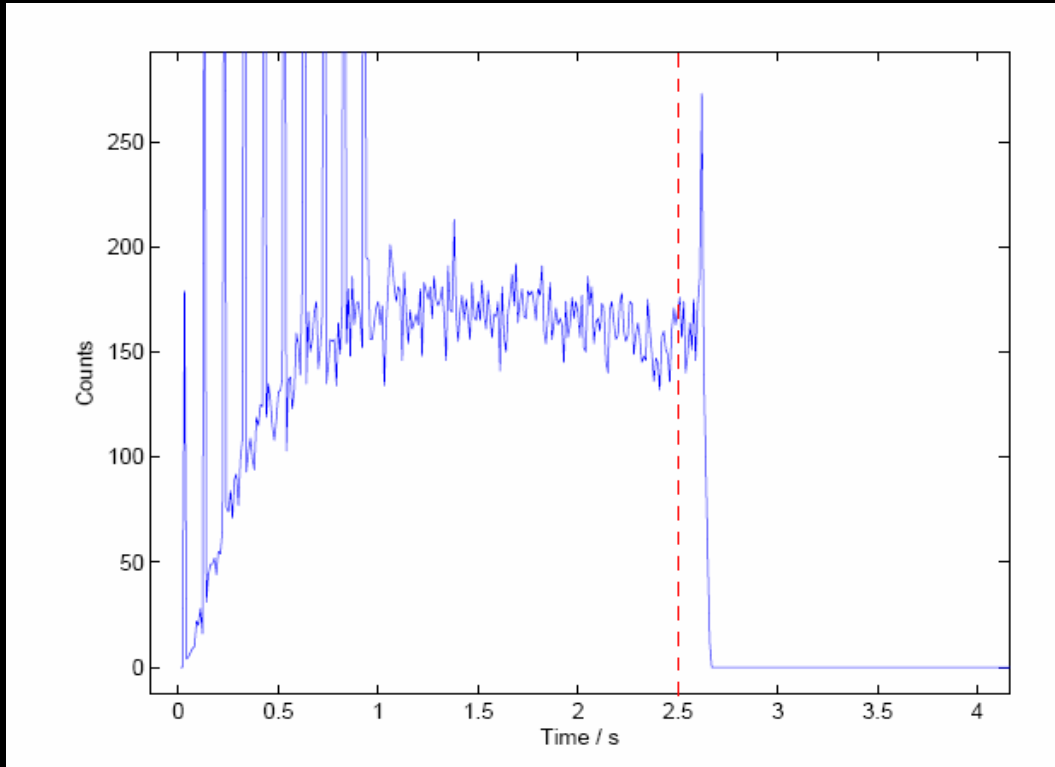
Conditions: Fe^{24+} , Temperature 200eV, 250 V trap depth ramped at rate of 1 kV/sec. All other mechanisms (ionization heating, e-beam heating, and cooling by collisions with low-Z ions) ignored.

(a) and (c) are simulations for a trap to empty

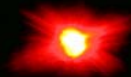
(b) and (d) are simulations for a trap depth ramped from 250 V to 50 V



Evaporative Cooling – Preliminary results



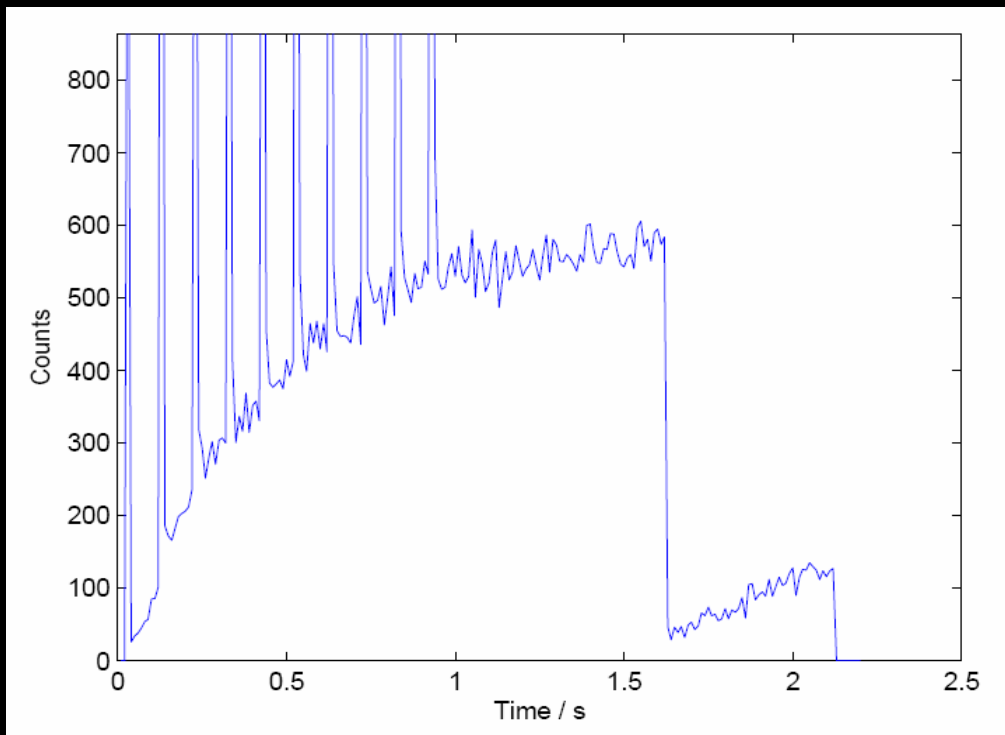
Evaporatively cooled Fe^{24+} . Initial trap depth = 250 V, Ramp rate = 1 kV/sec, Ramp start indicated by dashed line. Left hand plot is for ramp to inverted trap. Right hand plot is held at a trap depth corresponding to the time of the peak of the left hand plot (determined to be 53 V).



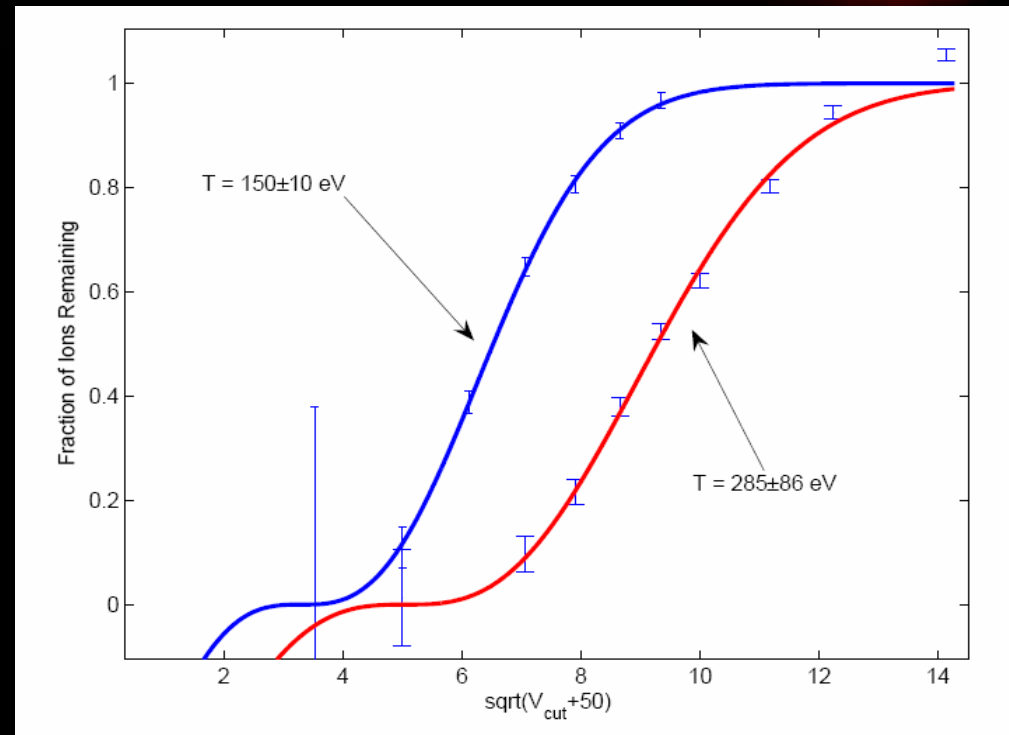
Work in Progress – Time resolved x-ray spectra to directly measure changes in Doppler broadening of ions



A Possible Qualitative Ion Temperature Diagnostic



Sudden change in axial trap executed at $t=1.6\text{s}$



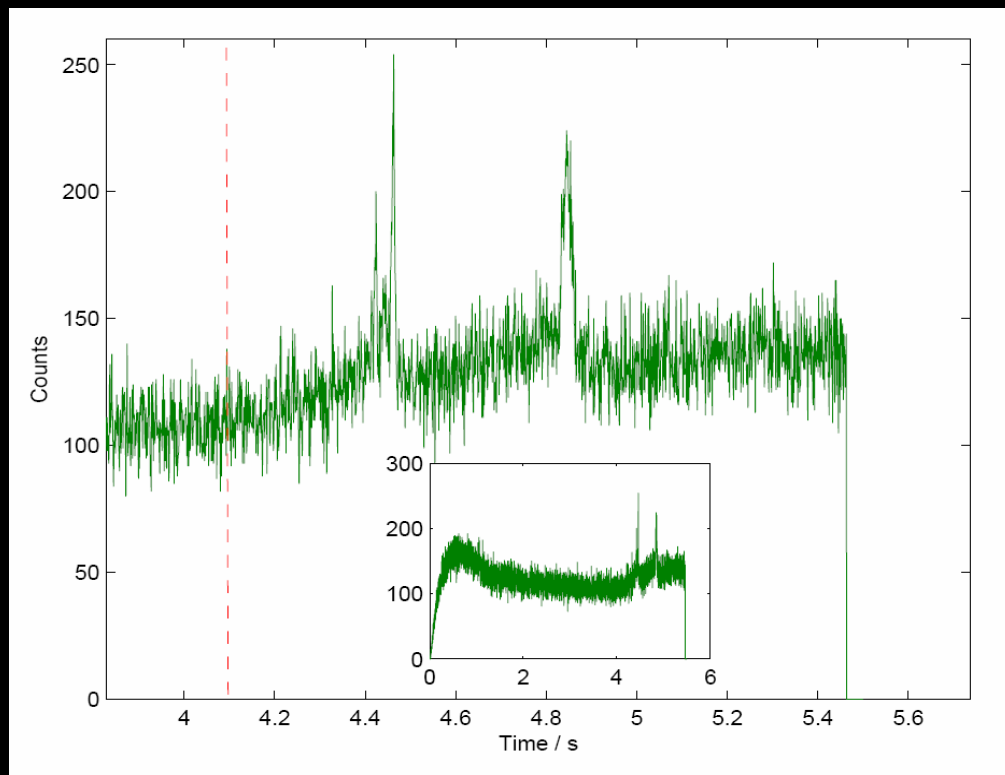
Blue curve: Trap initially set at 10V (+offset). Red curve: Trap initially set at 200V.

Sudden changes in the axial trap depth will lead to a sudden loss of ions from the trap. By measuring the size of the change in flux as a function of the size of the change in trap depth we can map out, in principle, the ion distribution function.

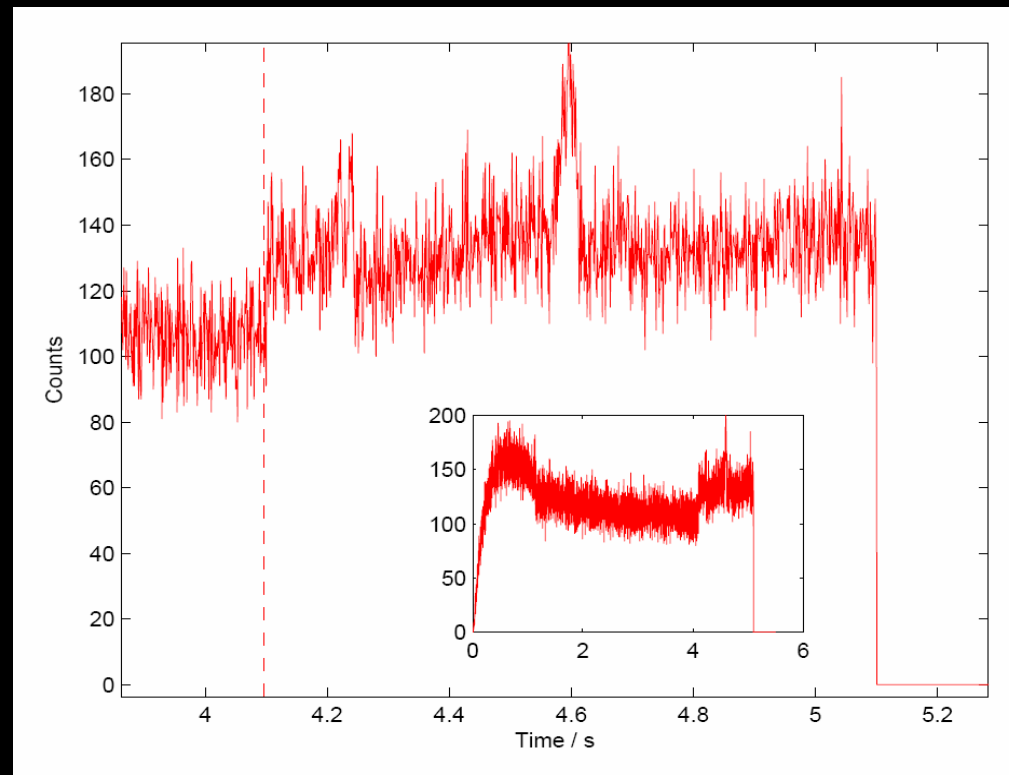
Or rather measure an effect which is correlated to the ion temperature. In fact the measurement is not instantaneous, the ion cloud will recover equilibrium on a \sim few ms, and the ion cloud-electron beam overlap factor will be different before and after.



Some Unexplained results



X-ray flux from H-like and He-like Argon when axial potential is reduced linearly from 500V to 137 V over 1 second.
12 keV, 50 mA electron beam.



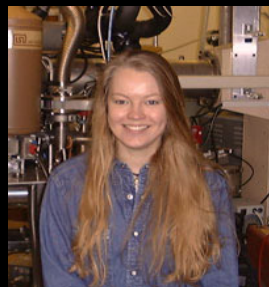
X-ray flux from H-like and He-like Argon when axial potential is abruptly switched 500V to 137 V.
12 keV, 50 mA electron beam.



The other OxEBITers



Josh Silver



**Kristina
Gaarde-Widdowson**



Toleme Ezekiel

Thanks also to...

Joshua Freeman (former undergraduate OxEBITer, now at Cambridge University)

Sohaib Shamim (former undergraduate OxEBITer)

Claire Smith (former OxEBITer, now at Cambridge University)

Kazu Hosaka (former OxEBITer, now at NPL),

Mike Tarbutt (former OxEBITer, now at Imperial College, London),

Peter Hirst (technician), Dr. Edmund Myers (Florida State University)

